# Preparation and Characterization of Noble Metal Single Crystal Electrode Surfaces


**Ludwig A. Kibler**

Department of Electrochemistry

University of Ulm

89069 Ulm, Germany

**http://www.uni-ulm.de/echem**

**e-mail: ludwig.kibler@chemie.uni-ulm.de**

# Preparation and characterization of noble metal single crystal electrode surfaces

## Preface

This booklet is an extract of several PhD theses and studies dealing with single crystal electrochemistry during recent years in the Department of Electrochemistry at the University of Ulm [Höl95,Dak96,Die96,Str98,Kib00]. In connection with short courses on "Preparation and Characterization of Noble Metal Single Crystal Electrode Surfaces" held at the 51st and 53rd annual meeting of the International Society of Electrochemistry, a short guide and reference work is presented in the following. We would like to share our experience with other electrochemical groups and to introduce scientists to the preparation techniques required for single crystal electrochemistry.

## Contents

## 1. Introduction

One of the main goals in modern electrochemistry, especially in the field of electrochemical surface science, is to establish relations between the surface structure of an electrode and its effect on a given electrochemical reaction, like metal deposition, adsorption of atoms, ions and molecules, oxidation of small organic molecules etc. These reactions are of utmost importance in electrocatalysis, especially when fundamental aspects of fuel cell reactions are investigated. The reason that single crystalline material is used for basic research is the rather complex behavior of polycrystalline surfaces, the structure of which cannot be easily controlled and characterized. Nevertheless, studies dealing with single crystal surfaces are sometimes contradictory and not always reproducible. We have gathered some rules that seem important to us in order to obtain and preserve well-ordered surfaces, starting from mechanically polished samples. With such surfaces it is possible by in situ techniques like STM to study the structure of noble metal electrodes on an atomic level, a basic requirement for going further into reactions and their kinetics.

This work concentrates on the preparation of well-ordered surfaces of noble metals, which are the elements of the platinum group plus silver and gold. For practical reasons, however, osmium will not be taken into account.

## 2. Surface structure of fcc-metals

The atoms in a single crystal are arranged in a three-dimensional periodic lattice. It can be built up by simple translation $\vec{t}$ of a unit cell, which is completely described by three vectors $\vec{a}_x$, $\vec{a}_y$, $\vec{a}_z$ (lattice constants) and three angles $\alpha$, $\beta$, $\gamma$ (Fig. 2.1)

$$\vec{t} = p\,\vec{a}_x + q\,\vec{a}_y + r\,\vec{a}_z \qquad \text{p, q, r: integer numbers}$$

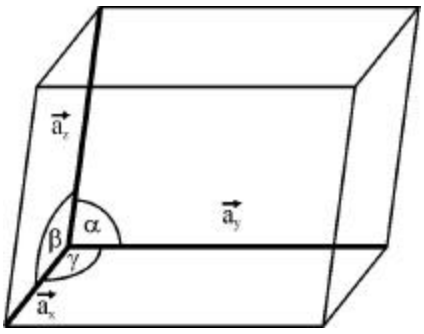


**Fig. 2.1:** General unit cell with lattice parameters.

The elements Ag, Au, Pd, Pt, Rh and Ir, which are considered in this work, all crystallize in an fcc (**fcc** = **f**ace **c**entered **c**ubic, see Fig. 2.2), Ru in a hcp (**h**exagonal **c**lose-**p**acked) lattice. In the former case, the atoms are cubic densely packed and it holds:

$$\vec{a}_x = \vec{a}_y = \vec{a}_z = \vec{a}$$

$$\alpha = \beta = \gamma = 90°$$

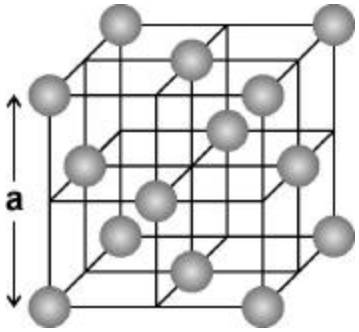


**Fig. 2.2:** Unit cell of a face-centered cubic system.

This structure is also characterized by stacking two-dimensional hexagonal close-packed layers in the sequence ABC, which recurs again and again (Fig. 2.3).

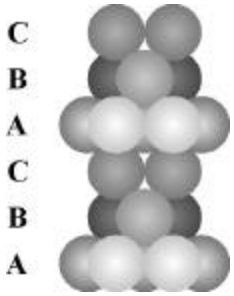


**Fig. 2.3:** Cubic densely packed ball model.

The faces of a single crystal are usually characterized by Miller indices (hkl). These represent the reciprocal of the intercepts of the plane under consideration with the x-, y- and z-axes. By convention, small integer numbers are used. Thus, parallel planes have identical indices. Negative intercepts are indicated with a bar above the respective indices. The three low-index planes (111), (100) and (110) of fcc systems are atomically flat with hexagonal, square and rectangular arrangement of the surface atoms, respectively [Zan88]. The (0001) plane of hcp systems has also a hexagonal arrangement of surface atoms.

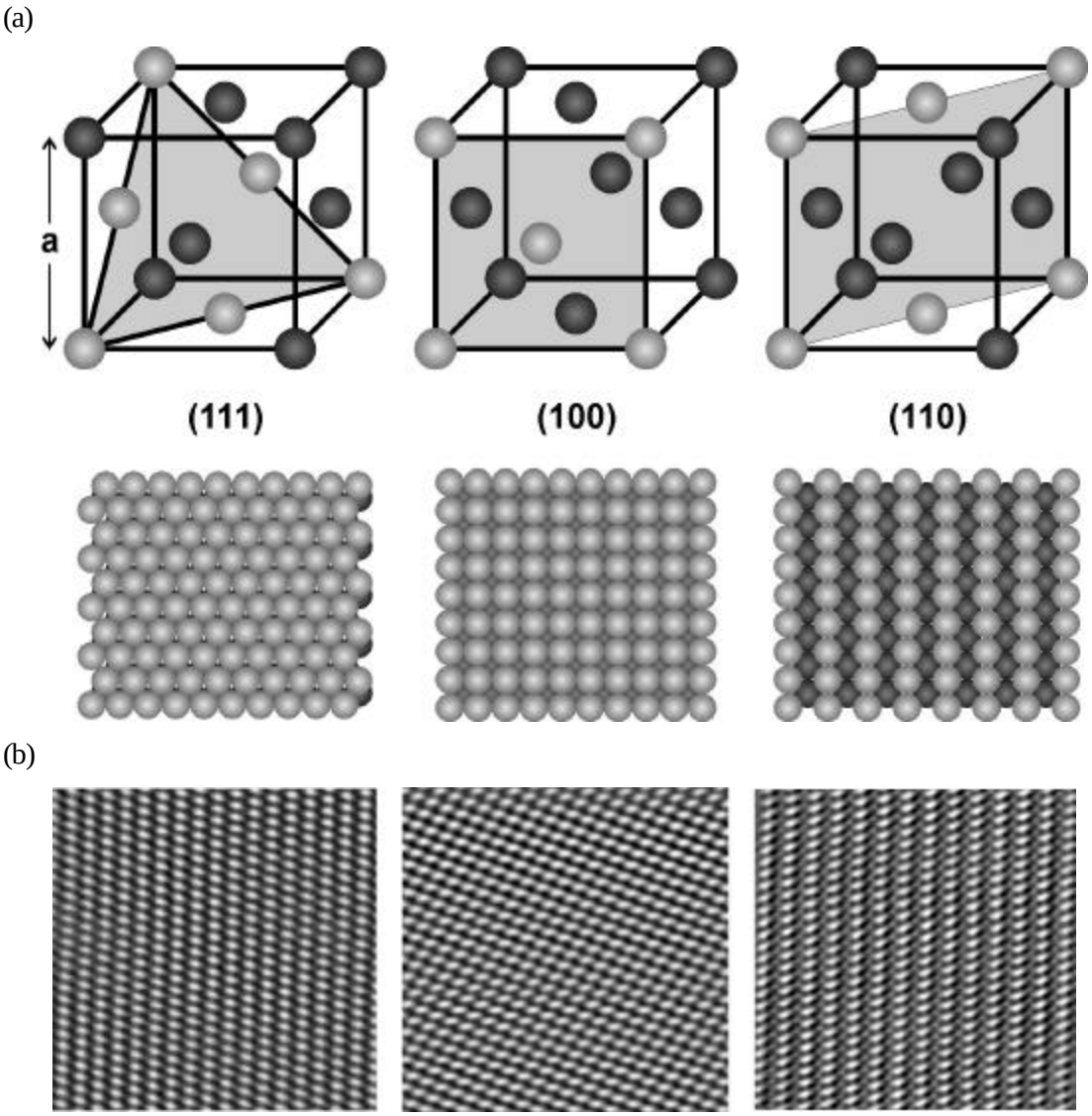


**Fig. 2.4:** (a) Ball models of the three low-index faces of an fcc-crystal. The atoms of the respective planes are shown more brightly. (b) High-resolution STM images of Au(111), Au(100) and Au(110). 8 x 8 $nm^2$.

So far, only symmetry characteristics of ideal single crystals have been considered. However, real crystals have defects in their bulk, such as point defects, dislocations or mosaics [Mat00]. Due to these bulk defects and technical limitations in cutting and polishing, there are always inhomogeneities and defects on single crystal surfaces [Bud96]. The most important surface defects are adatoms, islands, vacancies, holes, monoatomic high steps and screw dislocations. Step bunching, disordered regions and grain boundaries are sometimes observed on single crystal surfaces. However, they are signs of poor quality and often originate from inexpert fabrication or improper handling.

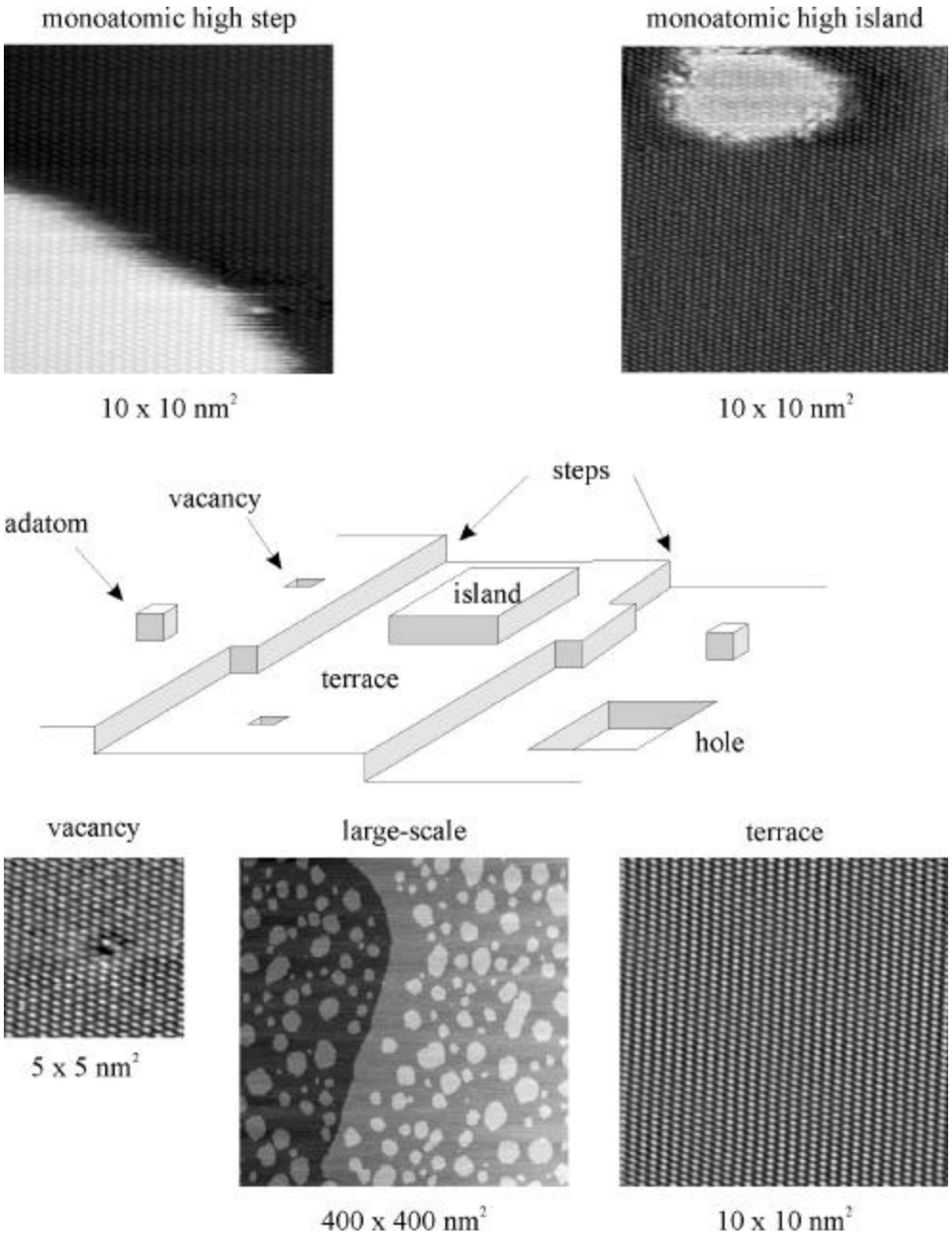


**Fig. 2.5:** *Kossel* crystal and selected STM images showing atomically flat terraces and various surface defects.

In Fig. 2.5, a simple model of a real surface and typical STM images are shown. As indicated above, a main cause for the existence of steps on a single crystal surface is a (small) misorientation as a result of cutting and polishing [Som94]. Sometimes such a miscut is formed willfully, in order to obtain surfaces with nearly equidistant monoatomic high steps and terraces of a certain average width. For (111)-surfaces, there are two different types of

close-packed steps. The geometry of theses steps can be {111} or {100}, the former being more stable than the latter ones [Mic91].

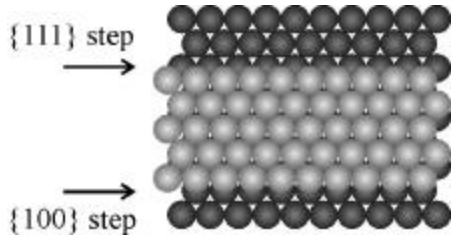


**Fig. 2.6:** {111} step and {100} steps on a (111)-surface.

The geometric arrangement of surface atoms usually deviates from that one of bulk atoms, since the coordination spheres are different. The distance between the first and second surface layer is often changed. This phenomenon is called surface relaxation [Tit96]. The two-dimensional atomic surface structure is not changed by surface relaxation [Kit89].
However, in some cases (Pt, Ir and Au), also the lateral arrangement of surface atoms can deviate from the bulk structure. This so-called surface reconstruction, which is driven by a lowering of the surface energy, is often connected with a phase transition and can be explained by the Smoluchowski effect [Smo41]. Typical examples for reconstructed surfaces are discussed in section 5. Even if the reconstructed surface is more stable than the unreconstructed one, the spontaneous transition into the reconstructed phase is often kinetically hindered at room temperature. The activation barrier can be overcome by thermal energy, i.e. by annealing (thermally induced reconstruction). Reconstruction of metal surfaces is a well-known phenomenon in an ultra-high vacuum (UHV) environment. Under certain experimental conditions, reconstructed surfaces are also stable in an electrochemical environment [Kol96]. At room temperature, examples for reconstruction induced by potential or adsorption are also well-known [Kol96].

## 3. Preparation of well-ordered noble metal single crystal surfaces

For all basic electrochemical investigations, we want to be able to prepare reproducibly well-ordered surfaces. Otherwise, the interpretation of measurements gets difficult or even misleading. Surface-sensitive techniques as described in section 4 will help in characterizing the quality of a metal surface. A well-ordered low-index surface must be atomically flat, having large terraces separated by monoatomic high steps and thus should possess as little other surface defects as possible.

Vacuum evaporation of noble metals on suitable substrates can give thin films of single-crystal quality (see section 5). The use of thin metal films supported on a conductive material is a convenient way to prepare electrocatalysts with high activity at low costs.

Massive metal single crystals are commonly grown by controlled cooling from a fluid phase. The growth process can be initiated by using a small seed crystal of the same material to define a crystallographic orientation and to avoid a supercooling of the fluid phase that could generate uncontrolled nucleation. The two most important growth procedures for bulk crystals are the Bridgman and the Czochralski method [Wil88].

By the Bridgman method the crystals can be grown by solidification in the temperature gradient region of a furnace whose temperature is decreased gradually. The Bridgman method is simple and cheap, although hampered by the problem of interference of the crucible with the crystallization process.

In the Czochralski method the crystal is pulled out of the melt by crystallization of the upper region of a meniscus. The growing crystal is visible and the growth process can be analyzed in-situ. The control mechanism which is required for proper shaping of the meniscus makes the method rather expensive.

In order to obtain a certain crystallographic orientation of the surface the single crystal must be shaped by mechanical sawing, spark or electrical discharge erosion or chemical erosion. Often, the shaping steps and the post-growth treatment are more difficult than the crystal growth process [Mat00].

X-ray diffraction is the main tool for the orientation of single crystals [Pre73]. Mounted to the head of a goniometer, the crystallographic orientation of a single crystal can easily be optimized by comparison of the Laue diffraction pattern with the so-called Greninger chart [Ham85]. By subsequent surface polishing (the crystal is usually embedded in epoxi resin) an accuracy of $<0.1°$ is achievable.

Polishing of the different crystals is to be performed very gently and where possible done chemomechanically. For pure mechanical polishing, at first, silicon carbide emery paper and afterwards diamond paste for hard materials or aluminum oxide for rather soft ones (Au) with

decreasing particle size for the different polishing cycles are used. By this, a surface roughness of better than 0.03µm can be obtained. Based on such a polishing procedure, an atomically smooth surface may be prepared within a few sputter- and heating cycles or by flame annealing, where remains of the polishing material are removed and the surface is smoothened [Mat00]. Given an orientation accuracy of <0.1°, terrace widths of several hundred nanometers are achieved. The quality and accuracy of mechanical polishing is crucial for obtaining well-ordered surfaces.

The small spherical single crystals, which are often used for the flame annealing and quenching method (see below) are usually prepared by melting one end of a high purity wire [Cla80a,Sas91b,Yau96,Dal99]. A well-prepared bead consists of (111) facets in an octahedral configuration. Such facets consists of large terraces, separated by monoatomic high steps and no other defects, and they can be directly used for STM experiments [Ita98]. In order to get other crystallographic orientations than (111), the small bead has to be oriented and polished.

## Methods for final preparation of single crystal surfaces

Single crystal surfaces can be prepared in **ultrahigh vacuum (UHV)** by cycles of Ar-ion bombardment and high-temperature-annealing (frequently in the presence of some oxygen) [Ros84,Hub88,Sor92]. By the use of surface science techniques (LEED, AES, XPS), the surface structure and the chemical composition of the surface can be examined in UHV just after the preparation. The transfer to an electrochemical cell and, after the experiment, back to the UHV chamber is possible, but this method is rather expensive and time-consuming. Still, UHV data are very important for structural characterization of single crystal surfaces. Even if there are sometimes discrepancies between observations in gas-phase and in electrochemistry, the characterization of UHV prepared surfaces provides indispensable details about clean and well-ordered structures that are generated by thermal treatment.

Clavilier, Faure, Guinet and Durand have shown in 1980 for the first time that the adsorption of hydrogen on Pt single crystal electrodes is strongly dependent on their crystallographic orientation [Clav80a,Clav80b]. Their major contribution is that they developed the very cheap and convenient **flame annealing and quenching method**, to handle Pt single crystals without the use of UHV techniques [Clav80a]. Small platinum electrodes with diameters of about 3 millimeter were annealed in a flame and afterwards immediately quenched in pure water. Using UHV-prepared Pt single crystals, it was later confirmed that the voltammograms of Clavilier et al. correspond to clean and well-ordered electrode surfaces [Abe86].

This flame annealing and quenching method was later also used for the preparation of Au [Ham85], Ag [Ham87a], Ir [Mot84a], Rh and Pd [Sas91a] single crystals. Especially for Pt and Au single crystals, the flame annealing and quenching method brought about a huge

variety of results and offered the possibility to work with single crystal electrodes for many electrochemistry groups all over the world. Recent reviews underline the importance of the easy handling of small single crystal electrodes [Cla91, Cla99,Ham96].

Before each experiment a single crystal has to be cleaned and the surface atoms have to be (re)ordered. Both is achieved by annealing in a flame. For this a Bunsen burner or a hydrogen flame can be used. Depending on the experimental problem several parameters can be varied:

-) oxidative or reductive zone of the flame

-) time

-) temperature

Single crystals are usually annealed in the oxidizing part of the flame in order to remove organic contaminants. The annealing period can range from seconds to hours. However, long-time annealing is only needed for healing rather disordered surfaces, but in this case, annealing in a small furnace at controlled temperature is more suitable. Thus, annealing periods of 1-2 minutes are frequently used and they are long enough to prepare reconstructed surfaces, for example.

It is obvious that heating above the melting point destroys a single crystal. The danger of melting is highest for silver and gold, since their melting points can easily be reached with a small Bunsen burner. For this reason, careful annealing demands moving the crystal repeatedly through the flame. Only high melting material can be held in a flame for longer time without any risk.

Annealing is very effective for freeing noble metal crystals from organic impurities, specially in the presence of oxygen. In any case, as soon as the sample is cooled down, it starts to be contaminated by the cooling atmosphere or by the laboratory environment. Of course this contamination process can be slowed down or even suppressed, if the surface is protected. There are different ways for the transfer from the electrode preparation environment to the electrochemical cell and depending on the experiment the best strategy should be found out for getting a clean and well-ordered surface in contact with the electrolyte.

The protection of the single crystal surface by a drop of Milli-Q water is a very common and suitable method for working under clean conditions. However, fast quenching (immediately after annealing) works only for small single crystals, i.e. small beads at the end of a wire, since they cool down relatively fast. When rather big crystals are used (diameter > 2 mm), quenching is known to destroy the bulk structure of single crystals due to the temperature shock, which induces large stresses [Mar86,Uch91]. Flame annealing and subsequent quenching of the crystal were found to increase the bulk mosaics, as measured by the full width at half maximum in X-ray diffraction, i.e. the bulk crystal is destroyed [Rob95].

Quenching also leads to an increase in surface defects like step dislocations [Kle00,Wan00] and the loss of reconstruction in the case of gold single crystals [Dak97].

Thus, when using single crystals, quenching must be avoided. Instead, the crystals have to be cooled in an gas atmosphere as clean as possible. After a sufficiently long cooling period, i.e. after the temperature of the crystal had fallen below 100 °C, a drop of Milli-Q water is attached to the surface for further protection without the danger of inducing surface defects. Experiments in our laboratory have shown, that this strategy leads to clean and well-ordered Ag and Au single crystal surfaces [Kol95,Dak99,Ebe00,Kib99,Kle99]. Due to different reasons, for the preparation of more active noble metals like Pd, Pt, Rh and Ir special precautions have to be made (see section 5).

Another annealing method outside an UHV chamber without the use of a flame consists in passing electric current through a single crystal. In combination with an **Iodine-CO replacement method**, an alternative to the flame annealing and quenching method for Pt single crystals has been reported [Hou87,Zur87]. The electrodes were cooled in iodine vapor and then transferred to an electrochemical cell, where the protecting iodine adlayer was replaced by CO. The subsequent stripping of CO left a clean and ordered Pt surface.

We have modified this procedure in two ways. First, by leaving out the iodine adsorption step, Pt single crystals can be cooled in a CO atmosphere directly after (flame) annealing. The surfaces are sufficiently protected by this simple **CO method**, which yields clean and well-ordered, unreconstructed Pt electrodes [Kib00a]. Secondly, active metals that are sensitive to oxygen can be annealed in an inert gas atmosphere by **resistive heating** [Cue99]. However, these two modifications are again limited to rather small single crystals (diameter <5 mm), because (i) for the formation of a complete CO monolayer that protects the Pt surface, longer cooling periods are needed and the danger of contamination increases with larger crystal dimensions and (ii) for resistive heating of rather big crystals high currents are needed, which may overheat the contact wires. In order to solve the latter problems, the crystals can be annealed in controlled atmospheres by **inductive heating**. This method is successfully used in our laboratory for preparation of noble metal single crystal surfaces [Aziz02,Kib02,Kib02b].

Occasionally, it was reported that **controlled anodic dissolution** of noble metals can result in the formation of well-defined surfaces [Ita99]. However, we assume that besides flat terraces also holes and other defects are created by such an etching process. Still, the flat and well-ordered surface parts may be used for STM studies.

## 4. Electrochemical characterization of single crystal surfaces

Well-prepared single crystal surfaces can be characterized by a variety of electrochemical methods. In any case, working under clean conditions is of highest importance. That`s why electrochemical cells must be made of material that can be thoroughly cleaned. Glass ware, Teflon or Kel-F is best immersed in conc. $H_2SO_4$ + 30% $H_2O_2$ (Caroic acid) for several hours and rinsed or boiled repeatedly with Milli-Q water. Solutions and chemicals of suprapure quality are standard. Ways have to be found out, to transfer clean electrodes to the electrochemical cell without contamination (see section 3).

For many electrochemical experiments, the freshly prepared electrode must be immersed into the electrolyte under potential control, for example to preserve the thermally induced reconstruction. The initial potential is often chosen to lie in the so-called double-layer region, where no Faraday reactions take place. Nevertheless, the electrode surface remains not always unchanged upon immersion into the electrolyte under potential control and hence it is an important task to determine in-situ the exact surface structure and its dependence on potential and solution composition.

**Cyclic voltammetry** is ideal for a first characterization of metal/electrolyte interfaces. Current-potential curves can be used as fingerprints and allow to quickly get a general idea of the surface quality. The potential of the electrode under examination is cycled between two potential limits at a constant scan rate. Plotting the measured current density against the electrode potential gives typical voltammograms [Sou90]. Fig. 4.1. shows a conventional electrochemical glass cell, like the ones we use in our laboratory. Note that only the oriented and polished surface of the working electrode is in contact with the electrolyte by the so-called dipping technique [Dic76].

Although cyclic voltammetry is a method, which averages information about the entire surface, it is indeed very sensitive. The cleanliness of an electrochemical system can be checked and the structure of the electrode surface can qualitatively be judged, provided that reference curves are available. There is not always consensus on what the really typical voltammetric features are. Extensive studies by different methods are often needed to determine in an unquestionable way, which voltammogram corresponds to the clean and well-ordered electrode surface.

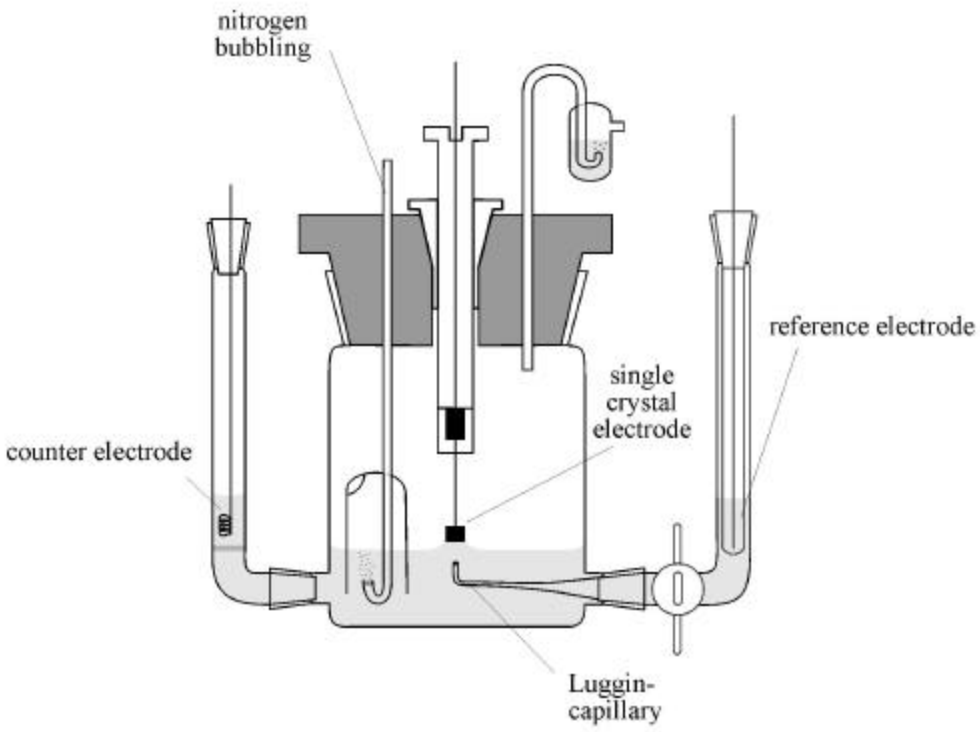


**Fig. 4.1:** Conventional glass cell for classical electrochemical measurements. The working electrode forms a meniscus with the electrolyte.

Even more sensitive than cyclic voltammetry are other classical electrochemical methods like **differential capacity measurements** or **impedance spectroscopy**. The latter belong to a.c. techniques, where the current response to a sinusoidal potential perturbation of certain frequency is analyzed [Sou90]. Briefly, important properties like the change of double-layer capacity with potential or the potential of zero charge can be determined by these methods.
After its invention in 1981 by Binnig and Rohrer [Gun91], **Scanning Tunneling Microscopy (STM)** was quickly adapted for electrochemical experiments [Son86] and soon became a powerful technique for the characterization of surfaces under potential control and for atomic-scale resolution. Many open questions concerning the actual surface structure of an electrode could be answered by STM in an impressive way due to imaging in real space. However, the combination of different surface-sensitive methods is still needed to fully describe a given electrochemical system.

## 5. Case studies

Concerning noble metal single crystal electrodes, a main focus has been on reconstruction phenomena of the electrode surface as a function of electrode potential and the adsorption of inorganic and organic species. To date, most of electrochemical studies have dealt with the three low-index Au and Pt surfaces. In the following, specific preparation techniques and typical results from electrochemical experiments are described.

### 5.1. Ag(hkl)

Silver is a soft, malleable metal with a characteristic silvery sheen when polished. It is stable against water and oxygen but is slowly attacked by sulfur compounds in the air to form a black sulfide layer. Silver dissolves in $H_2SO_4$ and $HNO_3$.

melting point: 961.9 °C
lattice constant: 4.08641 Å
atomic diameter: 2.890 Å

**Tab. 5.1:** Selected physical properties of low-index Ag surfaces

| | Ag(111) | Ag(100) | Ag(110) | Ref. |
|---|---|---|---|---|
| work function / eV | 4.74 | 4.64 | 4.52 | [Dwe] |
| potential of zero charge / V vs. SCE | -0.695 | -0.865 | -0.975 | [Val] |
| surface energy / $\mu Jcm^{-2}$ | 61.8 | 70.3 | 75.6 | [Liu91] |

It was reported that perfect, displacement-free Ag single crystal faces can be obtained by electrochemical deposition in a small capillary [Bud66].
Thin Ag films (5000 Å) on glass can be used as substitute for Ag(111) surfaces. Annealing of the film for 1-2 minutes at beginning red heat and cooling in inert gas leads to small (111)-terraces [Zei83].
For the preparation of massive Ag single crystal surfaces, chemical etching and flame annealing can be used [Bew75,Die96,TW95]. Chemical etching is especially necessary, when the Ag surface is (partly) white and dull.
The Ag crystal is dipped for 5 seconds into a freshly prepared 1:1 mixture of 0.42 M aqueous NaCN and 30% $H_2O_2$. Held in air for 15 seconds, the crystal gets brown under gas evolution. It is subsequently dipped for another 5 seconds in 0.76 M NaCN, where the silvery sheen reappears. Afterwards, the crystal surface is dried from its back by a paper tissue and the etching cycle is repeated three times. Rinsed thoroughly with Milli-Q water, the crystal has to

be completely dried in a nitrogen stream and carefully annealed in a hydrogen flame at dim red heat and cooled in nitrogen.

The surfaces that are obtained by this method are clean and atomically flat. Due to the etching, there is a loss of material and a rather high density of monoatomic deep holes and screw dislocations. The holes can be removed in-situ at potentials near Ag dissolution, where the mobility of the surface atoms is increased.

Since halogen adlayers on Ag(111) are stable in air, they can be used for protecting clean silver surfaces against contamination during transfer [Sch94]. However, such an intermediate step in surface preparation is not necessarily needed. After annealing, cooling in air is only possible for small crystals [Sch94]. Otherwise an inert atmosphere (nitrogen or Argon) has to be used [Ham87a].

A serious problem with flame annealing of silver is the formation of a white dull surface, which indicates a certain roughening. This happens occasionally and cannot easily be avoided, when silver is flame annealed. For this reason, frequent chemical etching is used for getting back a shiny, mirror-like surface.

It was observed, that annealing the Ag single crystal just above the flame instead of moving it in the flame, does not cause these problems [Ebe00]. In this way, high surface quality is achieved and more reproducible results are obtained.

Recently, clean and well-ordered surfaces were obtained by inductive heating of chemically etched Ag single crystals in an $Ar+H_2$ atmosphere [Schw02]. The surface quality can be preserved for a long period of time by using this method.

## 5.2. Au(hkl)

Gold is a soft metal with a characteristic shiny yellow color. It has the highest malleability and ductility of any element, and can be beaten into a film of micron thickness. Gold is unaffected by air, water, acids (except aqua regia, $HNO_3$/HCl) and alkalis.

melting point: 1064.4 °C
lattice constant: 4.0786 Å
atomic diameter: 2.884 Å

At room temperature, all three low-index Au surfaces are stable in their reconstructed phases.

Au(111)-($\sqrt{3}$ x22) [Bar90]
Au(100)-(hex) [Fed67]
Au(110)-(1x2) [Bin83,Rob84,Mor85,Möl86]

There are large discrepancies for the work functions of Au(hkl) in the literature. It is not always clear, if the reconstructed or the unreconstructed surfaces were measured.

**work function** / eV

| | |
|---|---|
| Au(111) | 5.30 ± 0.05 [Lec90], 5.20 [Val82b], 5.26 [Han78], 5.31 [Pot75] |
| Au(100) | 5.00 [Val82b], 5.22 [Han78], 5.47 [Pot75] |
| Au(110) | 5.12 ± 0.07 [Lec90], 4.8 [Val82b], 5.37 [Pot75] |

For each gold face, different values for the potential of zero charge were reported by different groups [Ham87b]. One of the reasons might have been that different preparation methods were used for the experiments. The pzc values of Kolb and Schneider are reproducible and were obtained for well-ordered surfaces. In the case of Au(110) there is some uncertainty due to a lack of surface characterization.

**potential of zero charge** / V vs. SCE [Kol86]

| | |
|---|---|
| Au(111)-(1x1) | 0.23 |
| Au(111)-($\sqrt{3}$ x22) | 0.32 |
| Au(100)-(1x1) | 0.08 |
| Au(100)-(hex) | 0.30 |
| Au(110)-(1x1) | -0.02 |
| Au(110)-(1x2) | -0.04 |

Mono-crystalline thin films of Au(111) can be grown on scratch-free mica. Flame annealing of the films removes contaminants, increases the flat surface area by a factor of 25 and produces the (22x $\sqrt{3}$ ) reconstruction of Au(111) [Dis98].

Au films (ca. 200 nm thick) evaporated onto special glass, with a thin Cr interlayer to improve Au adhesion, and annealed at 1000 °C produce compact films with large atomically flat (111) terraces [Hai91,Bat92,Bat95].

Flame annealing of a Au film, which was evaporated onto the base plane of a silicon hemicylindrical prism, produced a discontinuous film with crystallites terminated by a hexagonal pattern (60-90 nm) [Sun99]. These films facilitate the excitations of plasmon modes of the metal, resulting in surface-enhanced IR absorption.

Epitaxially grown Au overlayers on a well-ordered NaCl(100) surface were reported to behave similarly to a Au(100) surface [Lec78].

There are different methods for chemical or electrochemical cleaning and polishing of gold. In any case, etching should be avoided, because the surface defect density is increased.

However, electrochemical polishing is necessary to remove irreversibly adsorbed species like foreign metals or material from mechanical polishing.

-) chemical cleaning with boiling $HNO_3$ [Rob95]
-) electrochemical etching in a 1:1:2 mixture of glycol + ethanol + conc. HCl at 4.5 V [Rob92]
-) electrooxidation in chloride-free 0.1 M $H_2SO_4$ at 10 V and 0.2-0.3 $Acm^{-2}$ with a graphite counter electrode for 20 seconds, where a brown overlayer of gold oxide is formed. The oxide is dissolved by dipping for 2 minutes in 1 M HCl . This procedure is known to produce well-ordered terraces, but also step bunching.
-) electrochemical etching with cyanide [Teg56]. The electrolyte contains 6.7 g KCN, 1.5 g KNa-tartrate, 1.5 g $K_3Fe(CN)_6$, 2.25 g solid $H_3PO_4$ and a few drops of conc. $NH_3$ in 100 ml Milli-Q water. As a cathode stainless steel is used with a surface 10 times higher than the surface of the gold anode. The current density is set to 1.5 $Acm^{-2}$ at 70 °C. The quality of the surface should be controlled from time to time with a light microscope. There is a considerable loss of material, but this method was reported to give big, flat terraces [Bat94].

Flame annealing is very common and most suitable for preparing well-ordered Au single crystal electrodes. It is clear from AES and XPS data that flame annealing does not oxidize the gold or deposit soot on the surface [Dis98]. Furthermore, surface carbon and organic molecules can be removed by flame annealing. Au single crystals are usually annealed in the blue flame of a Bunsen burner or in a hydrogen flame for 2-3 minutes at red heat. The crystal has to be moved repeatedly through the flame so that heating above the melting point can be excluded. Cooling without any precautions leads to slightly dirty surfaces. Either the crystal is cooled in a stream of inert gas or it is cooled down in air, but just above the surface of Milli-Q water. The crystal has to be cooled down below 100 °C, before being brought in contact with water, i.e. any quenching has to be avoided. After the cooling period, which is determined by the size of the crystal, a drop of Milli-Q water is attached to the surface or the electrode can be directly immersed into the electrolyte under potential control. In the latter case, the dewetting of the walls of the crystal can take a lot of time and we prefer dipping the crystal protected by the water drop only after a waiting time of about 10 minutes, when it really has reached room temperature. By using this procedure, the thermally reconstructed surfaces are preserved in the electrochemical environment at sufficiently negative potentials.

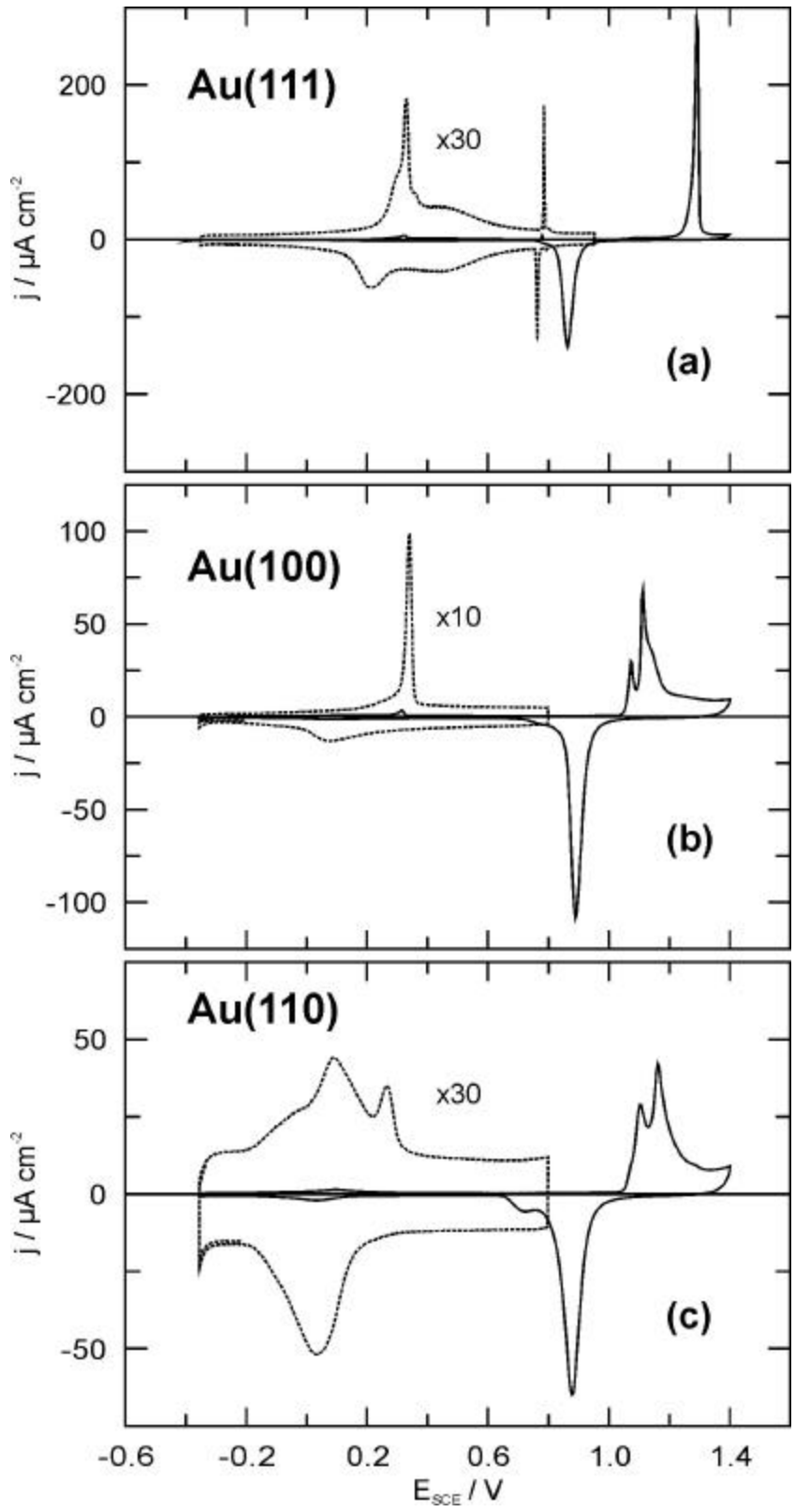


**Fig. 5.2.1:** Cyclic voltammograms for Au(hkl) in 0.1 M $H_2SO_4$, Scan rate 10 mV/s. The dotted curves are enlarged as indicated and represent the first cycles in the double layer region, starting at -0.2 V.

Fig. 5.2.1. shows cyclic voltammograms for the three low-index Au surfaces in 0.1 M $H_2SO_4$, which are often used to control the quality of the single crystals. At negative potentials, where no anions are adsorbed on the surfaces, the thermally induced reconstructed phases are stable in all three cases [Kol96]. The reconstruction is lifted at more positive potentials by specific adsorption of sulfate and the unreconstructed (1x1) surfaces are formed. This is indicated by the anodic current peaks at 0.34 V for Au(111) and Au(100). The anodic peaks positive of 1.0 V are due to gold oxide formation. These peaks can also serve as a check of the surface quality. After reduction of the oxide, however, surface defects like monoatomic deep holes are formed. Characteristic curves for Au(hkl) in contact with other electrolytes can be found in ref [Ham96].

**Au(111)**

The Au(111) surface is widely used in many fields of electrochemistry. This may be due to the large double layer region and the easy preparation of this surface. Both, the peak at 0.34 V for the lifting of the reconstruction and the sharp spike at 0.78 V in Fig. 5.2.1a can serve as sensitive indicator of the surface quality, as experiments with stepped Au(111) surfaces have shown [Höl95,Dre97,Kib00]. With increasing defect density, the peak for lifting of the reconstruction gets smaller and is shifted towards more negative potentials. Also the height of the current spike at 0.78 V is related to the average width of the Au(111) terraces. At this potential an ordered $\left(\sqrt{3}x\sqrt{7}\right)R19.1°$ structure of sulfate is formed [Mag92,Ede94].

Another electrochemical reaction that is very sensitive to surface quality of Au(111) is the underpotential deposition of Cu, which has been studied exhaustivlely by many groups [Höl95,Höl95a]. The formation of the first Cu monolayer on Au(111) proceeds in two steps, as indicated by two cathodic peaks at 0.21 and 0.08 V (Fig. 5.2.2). At first, an ordered Cu submonolayer with $^2/_3$ coverage stabilized by coadsorbed sulfate is formed. The more negative peak for the completion of the Cu monolayer is split, if the Au(111) terraces are large enough. This is due to different overpotentials for nucleation of Cu at steps and on terraces.

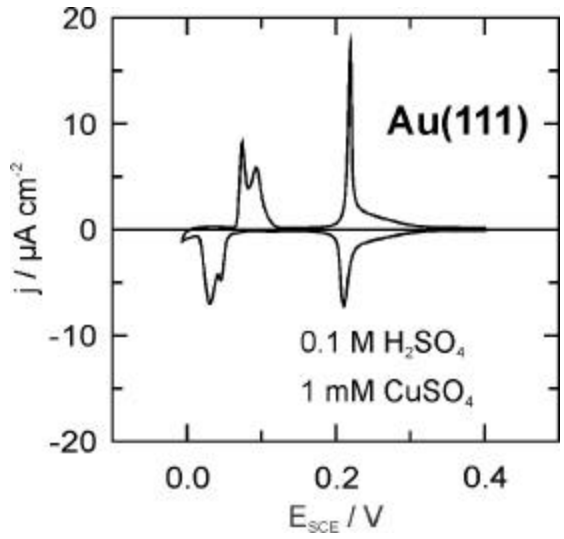


**Fig. 5.2.2:** Cyclic voltammogram for Cu underpotential deposition on a well-ordered Au(111) electrode in 0.1 M $H_2SO_4$ + 1 mM $CuSO_4$. Scan rate 1 mV/s.

**Au(100)**

Reconstruction phenomena at the Au(100)/electrolyte interface were studied in detail [Kol96]. A flame-annealed Au(100) single crystal electrode surface exhibits a hexagonal reconstruction and undergoes a reversible hex ↔ (1x1) transition in electrolyte [Gao91a,Gao92,Mag93b, Dak97]. On the unreconstructed Au(100) surface an ordered sulfate structure was observed by STM [Kle99].

**Au(110)**

Au(110) reconstructs into a (1x2) missing-row structure, where every second row in [001] direction is missing. The surfaces that were imaged by in situ STM after flame annealing of Au(110) are very rich of defects and not well-ordered [Mag93a,Gao91b]. For a freshly prepared Au(110) surface (1x1), (1x2) and (1x3) structures were observed at the same time in the double-layer region [Gao91b]. However, preliminary measurements in our lab have shown, that it is possible to preserve the (1x2) thermally induced reconstruction at negative potentials, which transforms into the unreconstructed (1x1) phase upon sulfate adsorption [Kle00]. From these measurements, it seems important for the preparation of Au(110) not to anneal the electrode at high temperatures. It is known that the Au(110) surface undergoes an order-disorder phase transition at about 700 K [Rom93,Stu96]. Thus, it is possible that the

rather rough surface structure is frozen after cooling and well-ordered surfaces are only obtained, if 700 K are not exceeded.

## 5.3. Pd(hkl)

Palladium is a lustrous, silvery-white, malleable and ductile metal. It resists corrosion, but dissolves in oxidizing acids and in molten alkalis. Palladium metal has the unusual ability of allowing hydrogen to absorb in its bulk. It is mainly used as a catalyst.

melting point: 1544 °C
lattice constant: 3.8898 Å
atomic diameter: 2.751 Å

Thermally induced reconstruction does not occur on Pd surfaces. However, a (1x1) $\rightarrow$ (1x2) transformation by CO, oxygen or hydrogen was observed on Pd(110) in the gas phase [Rav90,Tan95b,Yos95].
Pd single crystal electrodes were often electropolished in a solution of 0.5 M LiCl and 0.2 M $Mg(ClO_4)_2$ in methanol [Chi88,Bal96,Zou98]. This method was developed for Transmission Electron Microscopy of palladium [Sch75].
The flame annealing and quenching method was applied to Pd single crystals [Sas91]. Later, a cooling st ep by using a stream of inert gas was introduced [Sas96,Hos97,Wan00,Hos02]. We have observed, that after a few cycles of flame annealing, our rather big Pd crystals appear white and dull, indicating a certain roughening of the surface. It seems that the pr esence of oxygen in the flame destroys the crystals. For this reason, we prefer to anneal Pd single crystals in Ar or nitrogen atmosphere by resistive or inductive heating [Cue99,Aziz02,Kib02]. After a sufficiently long cooling period in the inert gas, the Pd surface is protected by Milli-Q water or by a drop of electrolyte.

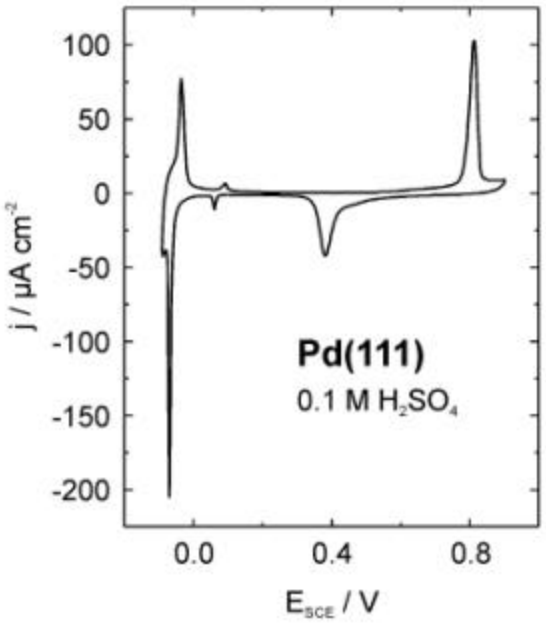


**Fig. 5.3.1:** Cyclic voltammogram for Pd(111) in 0.1 M $H_2SO_4$. Scan rate: 10 mV/s.

It was found that surface oxidation of palladium is strongly dependent on the crystallographic orientation [Sas96]. The adsorption of hydrogen on Pd is often masked by hydrogen a**b**sorption. However, the use of epitaxially grown Pd films on Au(hkl) or Pt(hkl) allows to study this reaction [Bal93,Llo93]. Voltammograms for hydrogen adsorption and oxide formation on stepped Pd single crystals are shown in refs. [Hos00,Hos02]. Pd single crystal surfaces show a rather broad double-layer region in sulfuric acid solutions and characteristic peaks in the hydrogen adsorption and oxide formation region (Fig. 5.3.1). The latter reaction causes a change in the surface structure [Sas91]. In the case of absorption of hydrogen into the palladium bulk, even the crystal lattice may be changed. In addition to voltammetry in base electrolytes, Cu underpotential deposition can be chosen to check the quality of Pd single crystal surfaces [Cue99,Oka01].

With in-situ STM, an atomically flat Pd(111) surface with monoatomic high steps was imaged [Sas91] and the formation of an ordered $\left(\sqrt{3}x\sqrt{7}\right)R19.1°$ structure of sulfate on Pd(111) has been observed [Wan00,Cue00].

## 5.4. Pt(hkl)

Platinum is a lustrous, silvery-white, malleable and ductile metal. It is unaffected by air and water, and will only dissolve in aqua regia ($HCl/HNO_3$) and molten alkalis. Platinum is used among others in jewelry, anti-cancer drugs and as catalyst.

melting point: 1772 °C
lattice constant: 3.9231 Å
atomic diameter: 2.774 Å

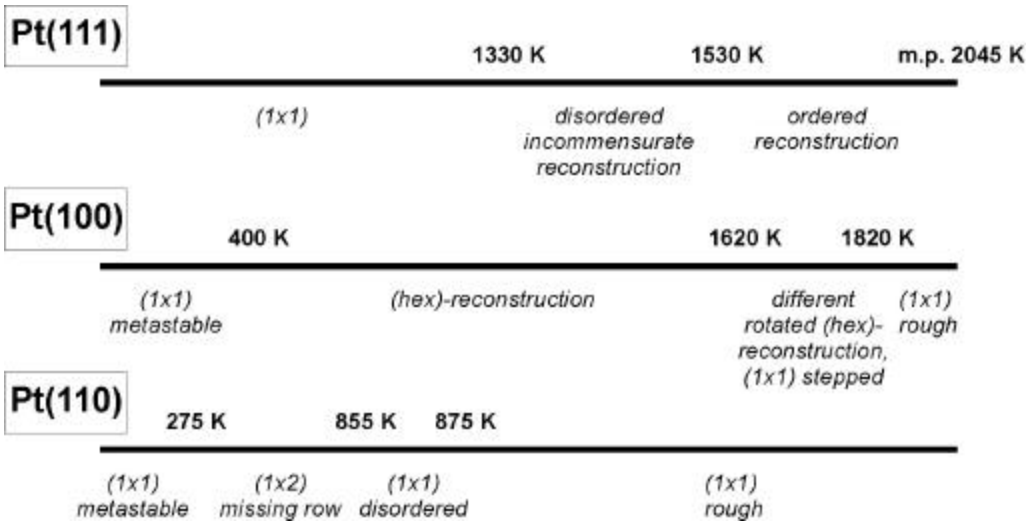


**Fig. 5.4.1:** Phase diagram for the three low-index Pt single crystal surfaces

Fig. 5.4.1 gives a quick overview for the stable phases of Pt(111), Pt(100) and Pt(110) surfaces in UHV at different temperatures [Bit96]. Except for Pt(111), which is reconstructed only at high temperature [San92,Bot93], these surfaces are reconstructed at room temperature:

Pt(100) -(hex) [Hov81]
Pt(110) -(1x2) [Bin83], [Mar83]

The annealing temperature is assumed to be important for obtaining well-ordered (reconstructed) surfaces, because high temperature phases may be frozen after fast cooling.
Electropolishing with a graphite counter electrode was reported [Bit96]: 2 seconds at 17 °C in 9:1 ethanol : 10% conc. HCl at 20 V and 2.5 A/cm$^2$. However, such a procedure does not seem necessary.

**Table 5.4:** Effect of different cooling atmospheres on the surface structure of Pt(hkl).

| | **Pt(111)** | **Pt(100)** | **Pt(110)** |
|---|---|---|---|
| air | furrowed, rough [a] | stripes, small islands, rough [b] | rough [c] |
| $N_2$ | well-ordered | reconstructed [d] | reconstructed [e] |
| $N_2$+$H_2$ | well-ordered | unreconstructed, islands [f] | well-ordered (?) [g] |
| $H_2$ | well-ordered, triangular step edges | many holes, some islands [h] | not measured |
| $N_2$+CO | well-ordered | well-ordered, unreconstructed [i] | unreconstructed [e] |

[a] *Clavilier et al. stress that cooling of Pt(111) in air does lead to a well-ordered and flat surface [Cla99]. In our opinion, this is only true for small single-crystalline beads, which cool down extremely fast.*

[b] *Stripes are running perpendicular to the step edges. They are separated by ca. 3.5 nm and consist of many small islands, which make the surface rich of defects [Kib00a].*

[c] *Cooling Pt(110) in air induces a high density of surface defects [Góm93]. Furthermore, oxygen seems to lift the (1x2) reconstruction [Bei95].*

[d] *UHV prepared Pt(100)-(hex) electrodes exposed to Argon were found by LEED/RHEED to be still reconstructed [Wu98]. Regarding the stability of Pt(100)-(hex) in electrolytic environment, to date there is no consensus [Zei94,Wu98,Akl99]. In-situ STM images present flat surfaces [Kib00a], however, neither reconstruction rows nor atomic resolution has been achieved yet.*

[e] *As suggested by Cu UPD and comparison with UHV prepared Pt(110) surfaces [Zei97, Kib00a].*

[f] *The islands (8-20 nm) appear similar to the islands obtained after lifting of the Au(100)-(hex) reconstruction [Kol96].*

[g] *The sharp peaks in the voltammogram might be related to a well-ordered (unreconstructed?) surface [Góm93], but a direct proof by in-situ methods cannot be given.*

[h] *Such an effect of a high concentration of hydrogen in the cooling gas has been reported by several groups [Cla94b,Fel94b,Kib00a]. Sashikata et al. have observed step lines with zigzag features and 45° angles [Sas98], which might be a result of quenching after cooling in a hydrogen stream.*

[i] *The excess platinum atoms originating from the lifting of the reconstruction do not create islands at elevated temperatures due to their enhanced mobility upon CO adsorption. On the other hand, CO dosing at room temperature after cooling in pure nitrogen gives rise to island formation [Kib00a].*

Since the seminal report of Clavilier et al., flame annealing is a widely used method for the preparation of Pt single crystals [Cla80]. The cooling conditions, especially the cooling atmosphere was seen to be crucial for the actual surface structure [Mot84c,Mar86]. Different surface structures as well as various stepped Pt single crystal surfaces give rise to distinct voltammetric profiles in the hydrogen adsorption region [Cla91,Mot87]. Recently, systematic STM studies have unequivocally shown the dramatic effect of a cooling atmosphere on the surface structure [Cla94b,Fel94b,Kib00a]. It should be noted again, that quenching the hot crystal must be strictly excluded, in order to avoid the additional creation of surface defects and a destruction of the bulk lattice. The effect of different cooling atmospheres is briefly summarized in table 5.4 (Ar in exchange of nitrogen leads to identical structures):

Fig. 5.4.2. shows voltammograms for Pt(111), Pt(100) and Pt(110) in 0.1 M $H_2SO_4$. The electrodes were flame annealed and cooled down in $N_2$ + CO for 15 minutes [Kib00a]. During the cooling period, protecting CO adlayers are formed, which are stable against oxidation by air in the case of Pt(111) and Pt(100). The CO layer blocks adsorption of hydrogen and anions. After oxidative removal of the CO adlayer at 0.6 V, typical voltammograms for clean, well-ordered and unreconstructed Pt surfaces are obtained. It shall be mentioned that we have obtained our best results by this CO method.

**Pt(111)**

The spike at 0.19 V in the voltammogram of Pt(111) in 0.1 M $H_2SO_4$ indicates a phase transition within the adsorbed anion adlayer [Sch84]. At potentials positive of this spike and negative of OH adsorption at about 0.5 V, the formation of an ordered $\left(\sqrt{3}x\sqrt{7}\right)R19.1°$ structure of sulfate on Pt(111) was observed by STM [Fun95,Fun97,Kle00]. The height and the sharpness of the spike are well-known criteria for the cleanliness of the system and for the quality of the Pt(111) surface [Cla99].

For Pt(111) electrodes, which were cooled in air, the cyclic voltammogram shows a smaller butterfly and additional peaks at -0.03 and -0.18 V for hydrogen adsorption at defect sites [Kib00a]. Fig. 5.4.3 shows voltammograms of two other systems, which are commonly used for characterization of Pt(111) electrodes.

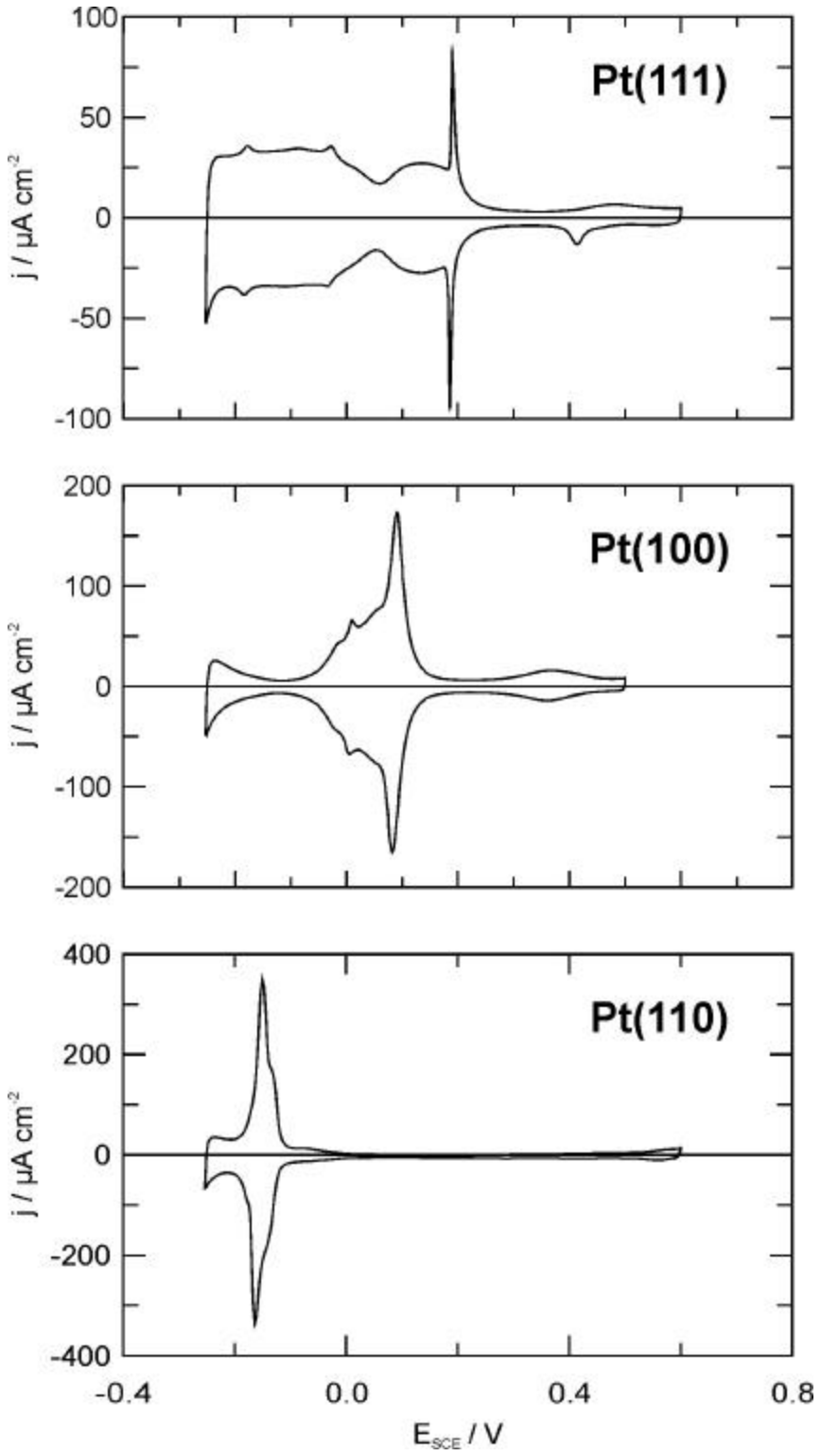


**Fig. 5.4.2:** Cyclic voltammograms for freshly prepared Pt(111), Pt(100) and Pt(110) in 0.1 M $H_2SO_4$ after cooling in a CO atmosphere and oxidative stripping of the CO adlayer. Scan rate: 50 mV/s.

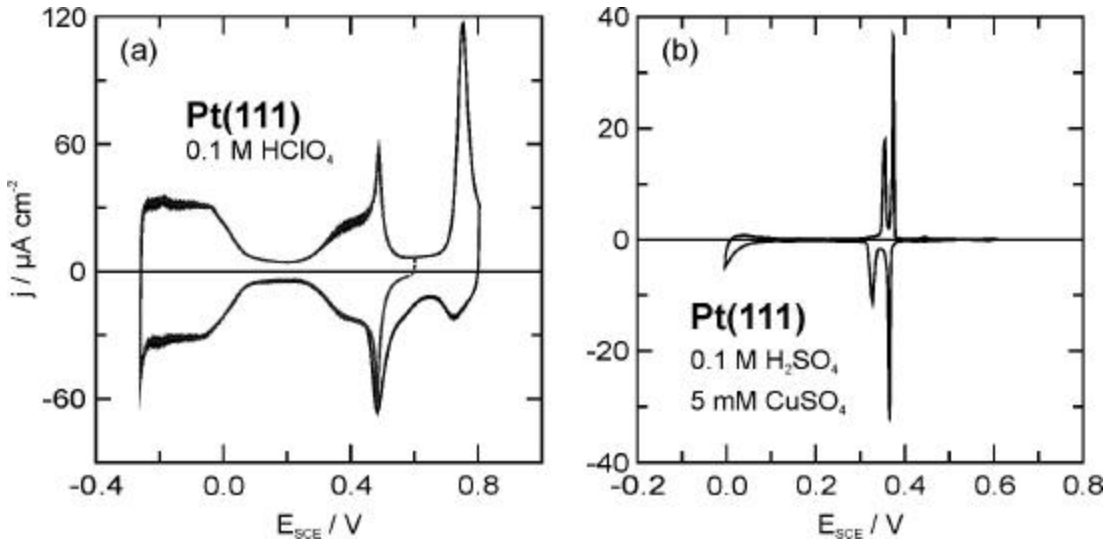


**Fig. 5.4.3:** Cyclic voltammograms for a well-ordered Pt(111) electrode a) in 0.1 M $HClO_4$, Scan rate: 50 mV/s and b) in 0.1 M $H_2SO_4$ + 5 mM $CuSO_4$, Scan rate: 1 mV/s.

For potentials negative of 0.1 V, voltammograms of Pt(111) in 0.1 M $HClO_4$ and in 0.1 M $H_2SO_4$ are identical. In both cases, the charge density for the hydrogen adsorption region amounts to 160 µC/cm$^2$. The peak at 0.49 V in Fig. 5.4.3a is ascribed to reversible OH adsorption [Wag83]. The subsequent oxidation step at 0.76 V is no longer reversible, however, current-potential curves are stable upon cycling to 0.8 V.

The voltammogram for Cu UPD on Pt(111) in Fig. 5.4.3b is similar to the curve for Cu UPD on Au(111) (Fig. 5.2.2). The UPD monolayer is formed in two distinct steps, but in a rather narrow potential window. Just between the peaks at 0.37 and 0.33 V, a $(\sqrt{3} \times \sqrt{3})R30°$ structure was imaged by STM [Sas91b,Mic92,Luc97]. As in the case of Au(111), a $^2/_3$ monolayer of Cu is stabilized by coadsorbed sulfate. Again, the sharp peaks are signs of good surface quality.

**Pt(100)**

As summarized in table 5.4, the Pt(100) surface structure is extremely sensitive to the cooling conditions after annealing. Fig. 5.4.4 shows cyclic voltammograms for Pt(100) in 0.1 M $H_2SO_4$ after cooling in different atmospheres. The height of the peaks at -0.02 and 0.08 V is changed systematically in the order CO, $H_2$, $N_2$ and air as cooling gases. According to Clavilier et al., the peak at -0.02 V is related to hydrogen adsorption at steps, while the peak at 0.09 V is characteristic for well-ordered Pt(100) terraces [Cla86,Cla89]. So-called CO charge

displacement experiments have shown that the charge densities in the hydrogen adsorption region include significant contributions of the adsorption of sulfate [Fel94a].

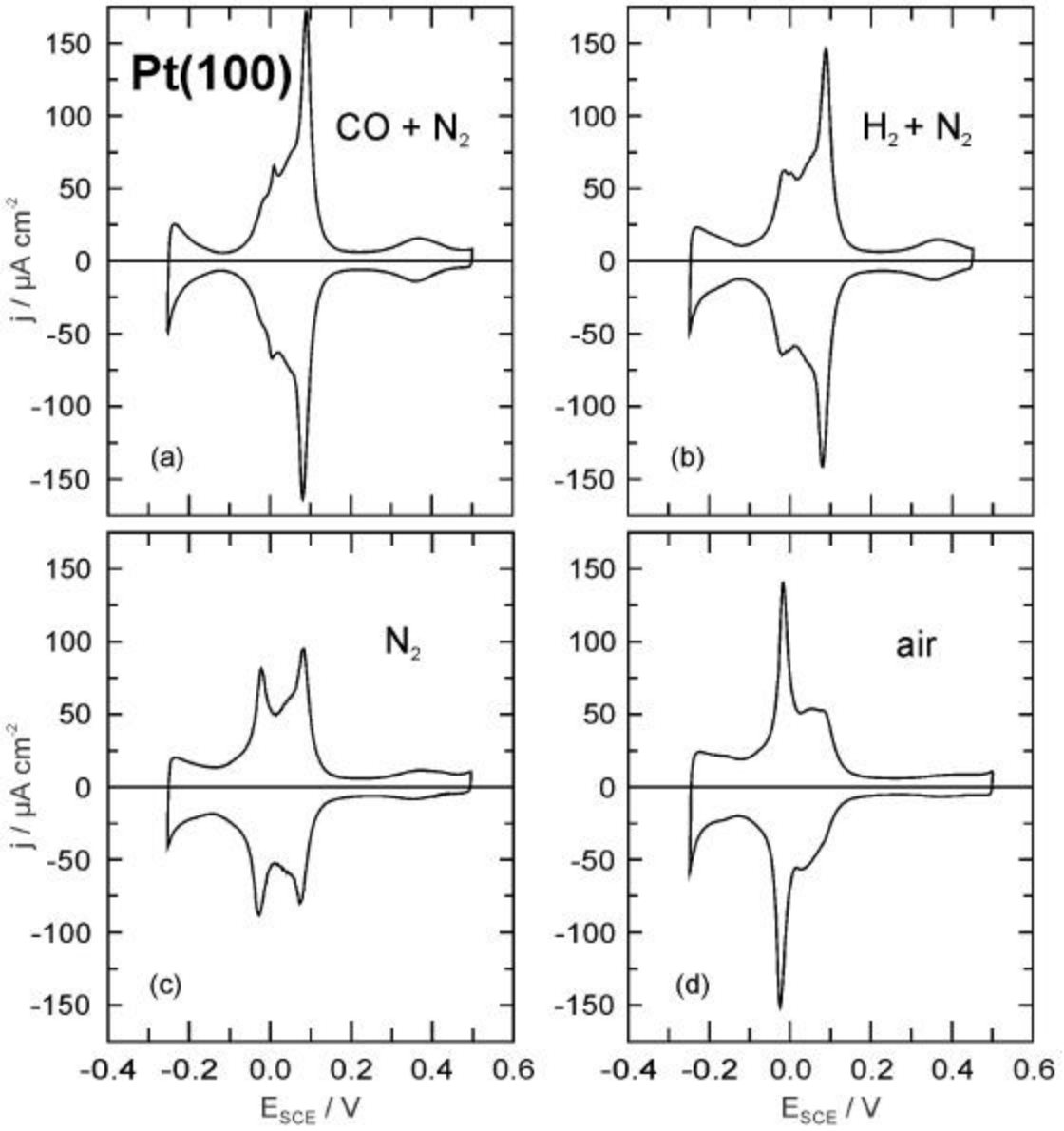


**Fig. 5.4.4:** Cyclic voltammograms for Pt(100) in 0.1 M $H_2SO_4$ after flame annealing and cooling in a) CO + $N_2$, b) $H_2$ + $N_2$, c) pure $N_2$ and d) air. Scan rate: 50 mV/s.

**Pt(110)**

Due to the relatively open structure of the Pt(110) surface and the existence of an order/disorder transition at about 800°C [Vli90], its preparation is rather difficult. It was reported that depending on the annealing temperature and the cooling period in Ar + $H_2$, either the (1x1) or the (1x2) structure was obtained [Mar97]. However, adsorbed hydrogen is

known to promote self-diffusion of platinum on the Pt(110)-(1x2) surface and partly lift the missing-row reconstruction [Hor99]. Thus, it is not clear, which structures are generated for Pt(110) after cooling in a hydrogen atmosphere and there is a lack of in-situ investigations in this respect. Fig. 5.4.5 shows voltammograms for Cu UPD on differently prepared Pt(110). As indicated above, there are good reasons, that cooling in nitrogen preserves the (1x2) structure and cooling in CO induces the lifting of the reconstruction by forming the (1x1) structure [Kib00a]. The curves for Cu UPD are more sensitive to the actual surface structure of Pt(110) than the voltammograms for hydrogen adsorption, which lies in a rather narrow potential window.

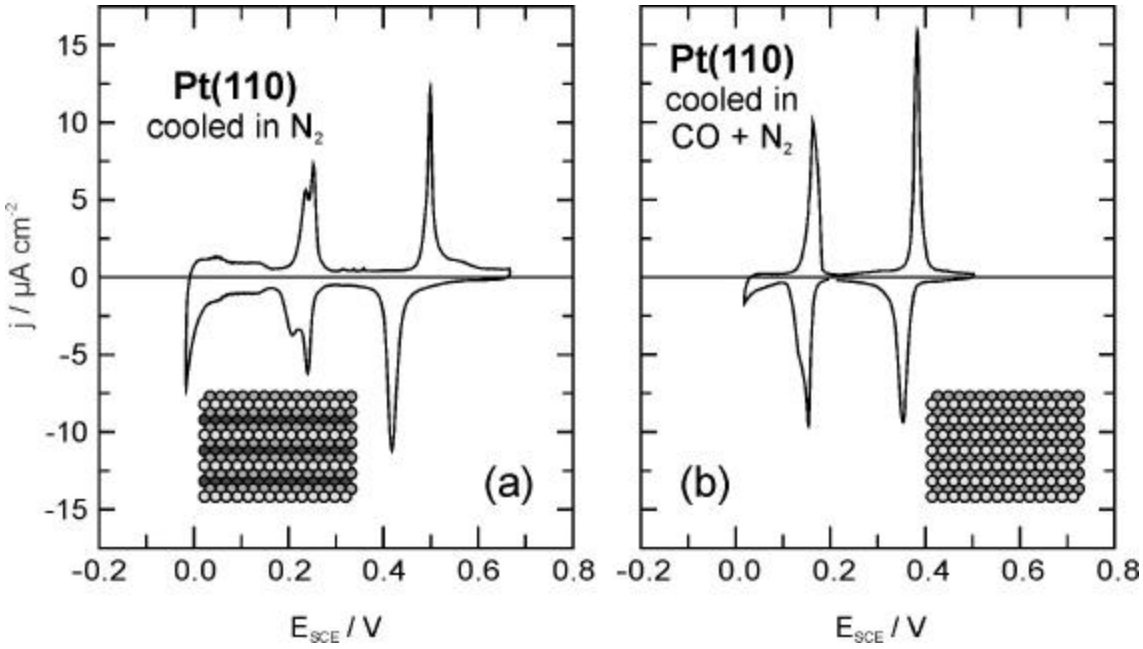


**Fig. 5.4.5:** Cyclic voltammograms for Cu UPD on a) reconstructed and b) unreconstructed Pt(110) electrode. 0.1 M $H_2SO_4$ + 5 mM $CuSO_4$. Scan rate: 1mV/s.

## 5.5. Rh(hkl)

Rhodium is a rare, lustrous, silvery, hard metal. It is unaffected by air and water up to 875 K, and unaffected by acids, but is attacked by molten alkalis. Rhodium is used as a catalyst.

melting point: 1966 °C
lattice constant: 3.8043 Å
atomic diameter: 2.690 Å

For some time, it was discussed, whether flame-annealing can be used for Rh single crystals or not [Leu89]. However, as for Pt single crystals, an oxygen-free cooling atmosphere is

necessary in order to avoid any roughening of the surface. Well-ordered Rh surfaces were obtained by cooling in a $H_2$/Ar-mixture [Cla94a,Wan95b]. Cooling in CO atmosphere also gives well-ordered Rh surfaces. However, it is not possible to oxidize the CO adlayer without structural changes.

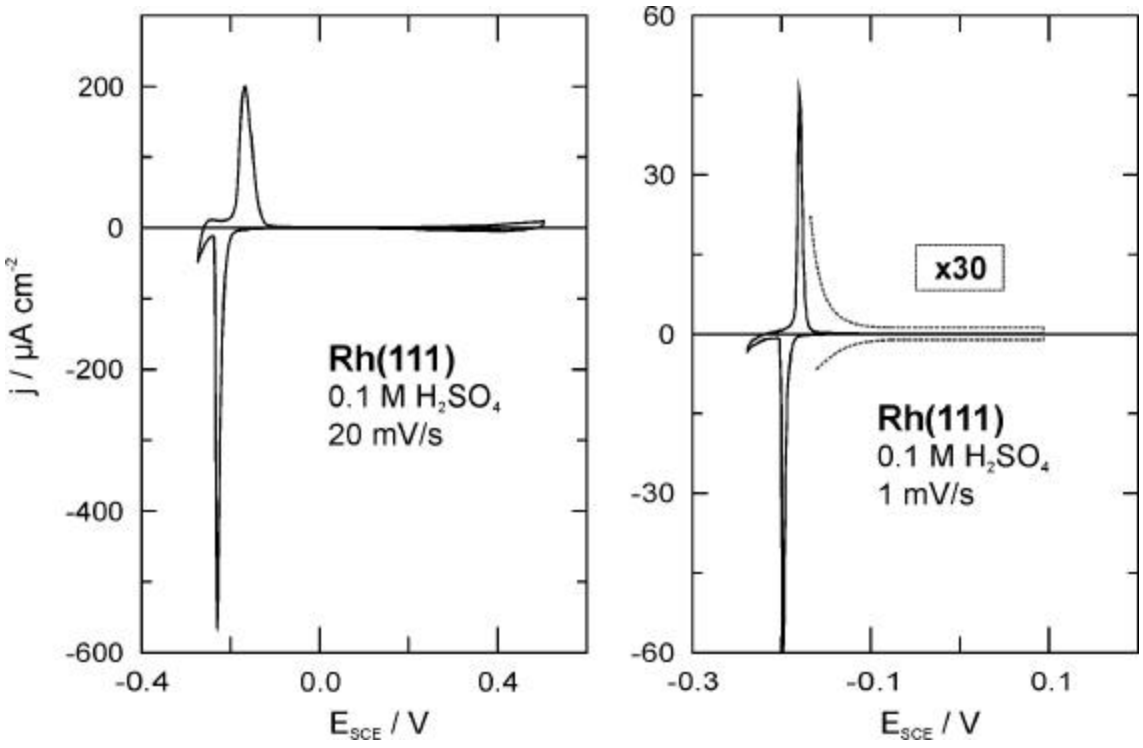


**Fig. 5.5.1:** Cyclic voltammograms for well-ordered Rh(111) in 0.1 M $H_2SO_4$. Scan rate a) 20 mV/s and b) 1 mV/s.

By using $N_2$ + $H_2$ as cooling atmosphere, we have obtained similar voltammograms for Rh(111) (Fig. 5.5.1) as described in the literature [Sun95,Góm97]. However, the formation of holes and islands was observed by STM [Cla94a], as in the case of Pt(100), when a high hydrogen concentration was used for cooling [Kib00a]. The voltammetric peaks in the hydrogen adsorption region at -0.2 V (Fig. 5.5.1) are coupled with anion adsorption. In the broad double layer region, the sulfate coverage is constant [Zel91] and a $(\sqrt{3}x\sqrt{7})$R19.1° structure of sulfate was observed by STM [Wan95b].

The strong interaction of Rh surfaces with anions is also reflected in the reduction of perchlorate [Rhe90]. The electrochemical behavior of Rh(111) in $HClO_4$ has been described in detail by Clavilier et al. [Cla94a]. There is almost no electrochemical study of Rh(100) and

Rh(110), but Rh(111) is frequently used in STM work and compared with Pt(111) [Yau96,Wan97].

## 5.6. Ir(hkl)

Iridium is a hard, lustrous, silvery metal. It is unaffected by air, water, and acids, but dissolves in molten alkali. Iridium is used in special alloys and spark plugs.

melting point: 2410 °C
lattice constant: 3.8394 Å
atomic diameter: 2.715 Å

Two of the three low-index faces of Ir are reconstructed in UHV. Ir(100) forms a quasi-hexagonal surface with a (5x1) superstructure [Hov81,Lan83]. Reconstructed Ir(110) belongs to the missing-row type and forms a (1x2) structure similar to Au(110) and Pt(110) [Cha86].

Motoo and Furuya have used Ir single crystal electrodes for the first time [Mot84a]. They have annealed the electrodes in the oxidizing zone of a propane-oxygen flame at ca. 2000 °C for 5 minutes and cooled down in pure hydrogen. The peaks in the hydrogen adsorption region were found to be strongly dependent both on the crystallographic orientation and on the anions present in the electrolyte [Mot84b].

The stability of reconstructed Ir single crystal surfaces in an electrochemical environment has not yet been studied.
Recently, the formation of an ordered $\left(\sqrt{3}x\sqrt{7}\right)$R19.1° structure of sulfate was observed on Ir(111) [Wan99].

## 5.7. Ru(0001)

Ruthenium is a lustrous, silvery metal of the so-called platinum group. It is unaffected by air, water and acids, but dissolves in molten alkalis. Ruthenium is used to harden platinum and palladium metals, and as a catalyst.
Melting point: 2309 °C
Crystal structure: hcp (a = 2.7058 Å, c = 4.2811 Å)

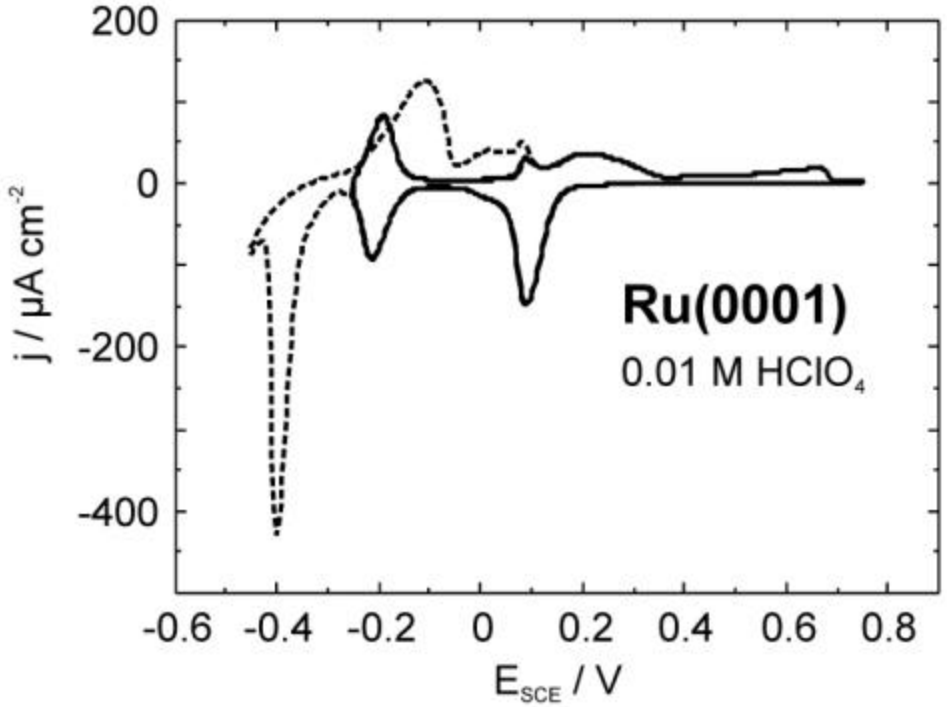


**Fig. 5.7.1:** Cyclic voltammograms for an inductively heated Ru(0001) electrode in 0.01 M $HClO_4$. Scan rate: 50 mV/s.

In low-temperature fuel cells, Ru is an important co-catalyst material for platinum anodes. Ru(0001) has been used in several recent studies as model surface to get a basic understanding about the catalytic properties of ruthenium electrodes on an atomic level. Ru single crystal electrodes have been prepared by annealing in ultrahigh vacuum (uhv) [Cao93,Lin00,Zei00,Lin00b,Mar00,Wang01,Mar01,Bra01,Wan01,Wan02,Lee02,Bra02].

Clean and well-ordered surfaces are also obtained by inductive heating in an argon stream [Kib02b]. Even by dipping the electrode into concentrated nitric acid followed by thorough rinsing with ultrapure water identical results were obtained. On the other hand, annealing and cooling in a hydrogen atmosphere [Bra02,Lu02] as well as simple mechanical polishing [Lu02] lead to significantly different curves.

A voltammetric peak in the hydrogen evolution region is ascribed to OH reduction and hydrogen adsorption, as suggested by CO displacement [Kib02b]. This peak is dependent on the pH of the solution and on the presence of specifically adsorbing anions.

## 6. STM gallery

(a) (b)

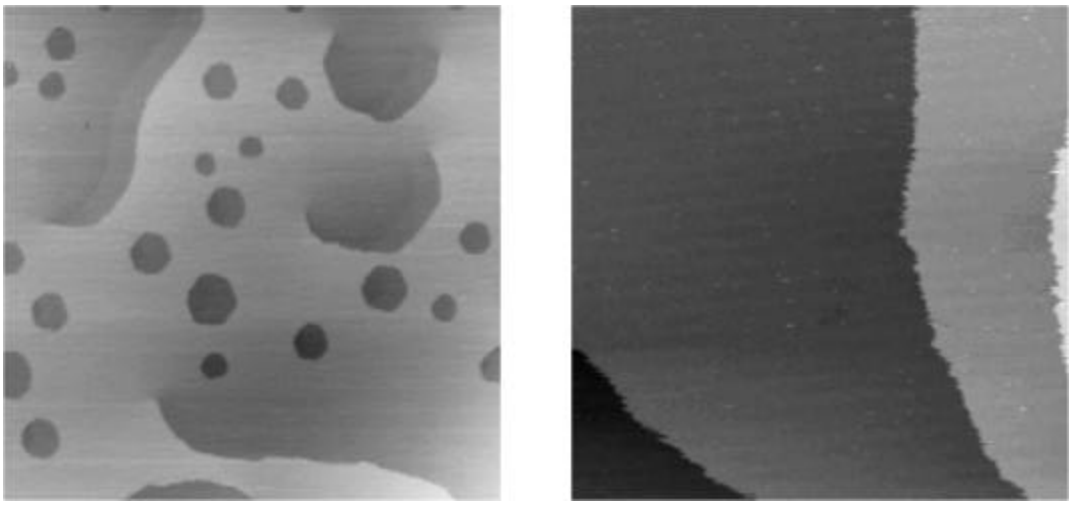

(a) STM image (500 x 500 $nm^2$) of an **Ag(111)** surface in 0.1 mM + 0.05 M $Na_2SO_4$ at E = -700 mV vs. SCE. The monoatomic deep holes are a result of chemical etching. They can be removed at positive potentials due to the increased mobility of surface Ag atoms. (b) STM image of well-ordered **Ag(110)** in 0.05 M $H_2SO_4$ + 1 mM $CuSO_4$ at E = 0.02 V vs. SCE. 150 x 150 $nm^2$. So-called *frizzy steps* demonstrate the high mobility of surface atoms. From ref. [Die96].

(a) (b)

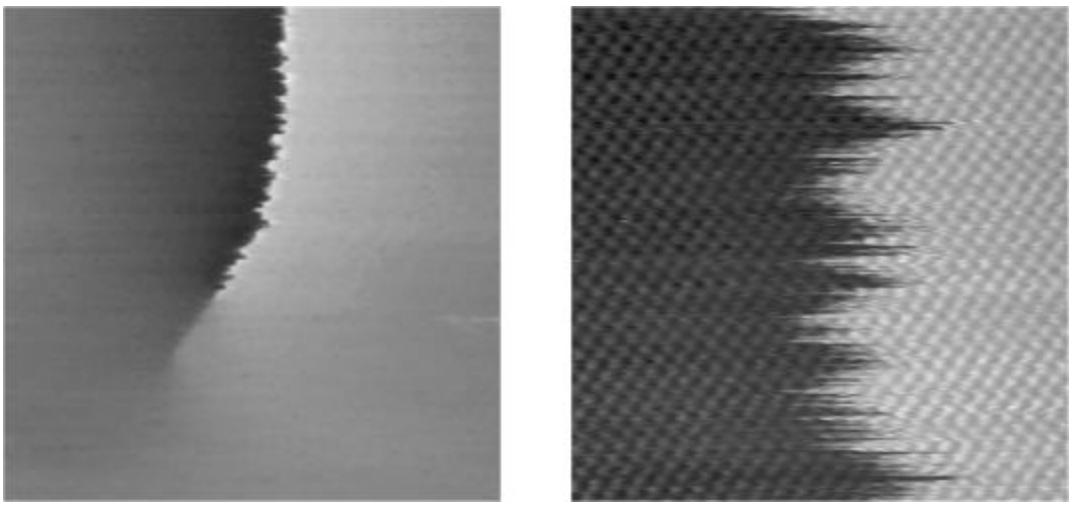

STM images of **Ag(100)** electrodes in 0.05 M $H_2SO_4$ + 1 mM $CuSO_4$ at E = 0.04 V vs. SCE. (a) Screw dislocation (50 x 50 $nm^2$). (b) Atomically resolved *frizzy step* (10 x 10 $nm^2$). From ref. [Die96].

(a) (b)

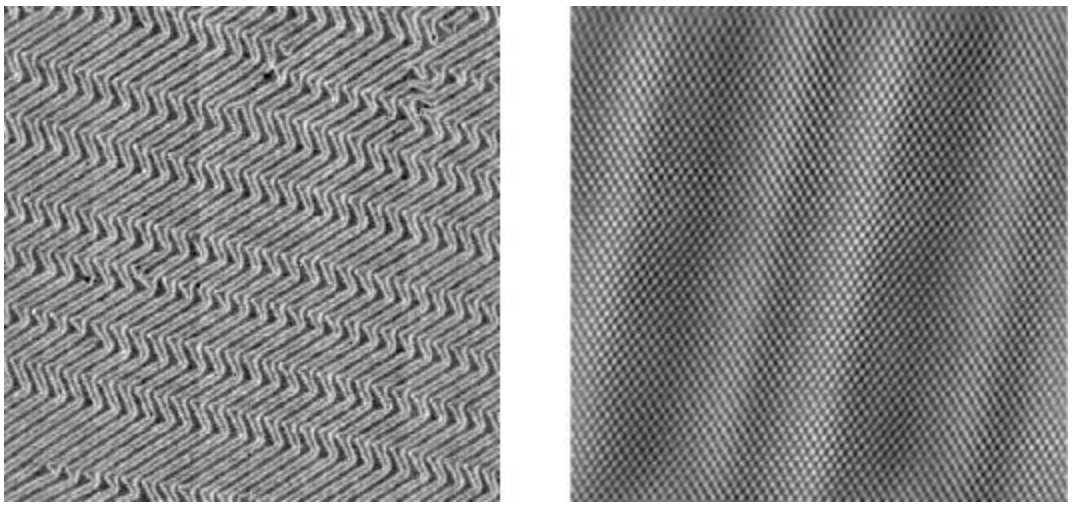

STM images of freshly prepared **Au(111)**-($\sqrt{3}$ x22) electrodes in 0.1 M $H_2SO_4$. (a) The reconstructed surface shows the well-known herringbone structure. E = -0.2 V vs. SCE. 200 x 200 $nm^2$. (b) High-resolution STM image. E = -0.2 V vs. SCE. 16 x 16 $nm^2$. Courtesy of M. Kleinert.

(a) (b)

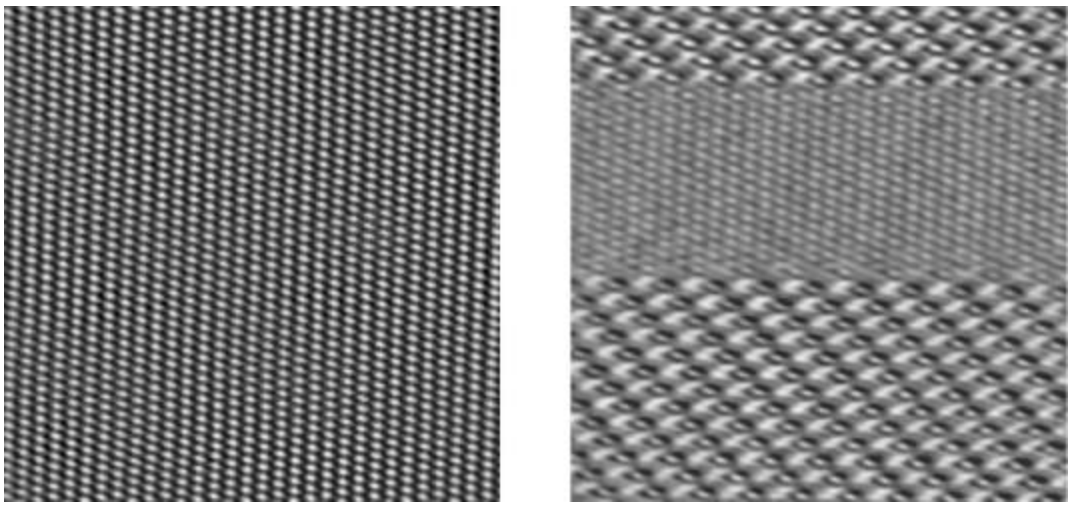

High-resolution STM images of unreconstructed **Au(111)** in 0.1 M $H_2SO_4$. (a) (1x1) structure showing the hexagonal arrangement of Au surface atoms. E = 0.55 V vs. SCE. 10 x 10 $nm^2$. (b) The ($\sqrt{3}$ x $\sqrt{7}$)R19.1° structure of (bi)sulfate on Au(111) is shown at E = 0.8 V vs. SCE (top and bottom of the STM image). The atomic structure of the substrate, which is seen at 0.65 V, can be used for internal calibration of the (bi)sulfate structure. Courtesy of M. Kleinert.

(a) (b)

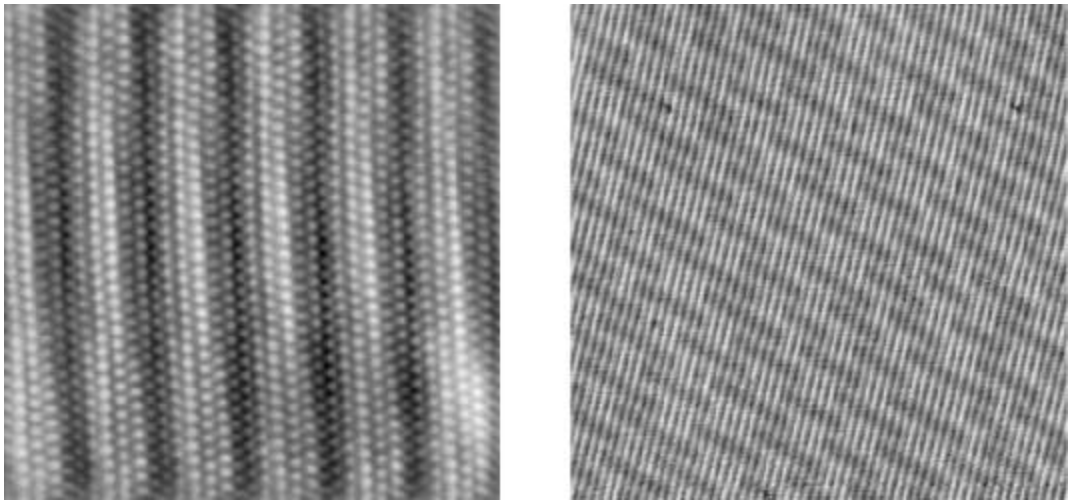

STM images of freshly prepared **Au(100)**-(hex) electrodes in 0.1 M $H_2SO_4$ at E = -0.2 V vs. SCE, showing (a) the reconstructed surface with atomic resolution (10 x 10 $nm^2$) and (b) a large-scale view of the reconstruction rows (100 x 100 $nm^2$). Courtesy of M. Kleinert.

(a) (b)

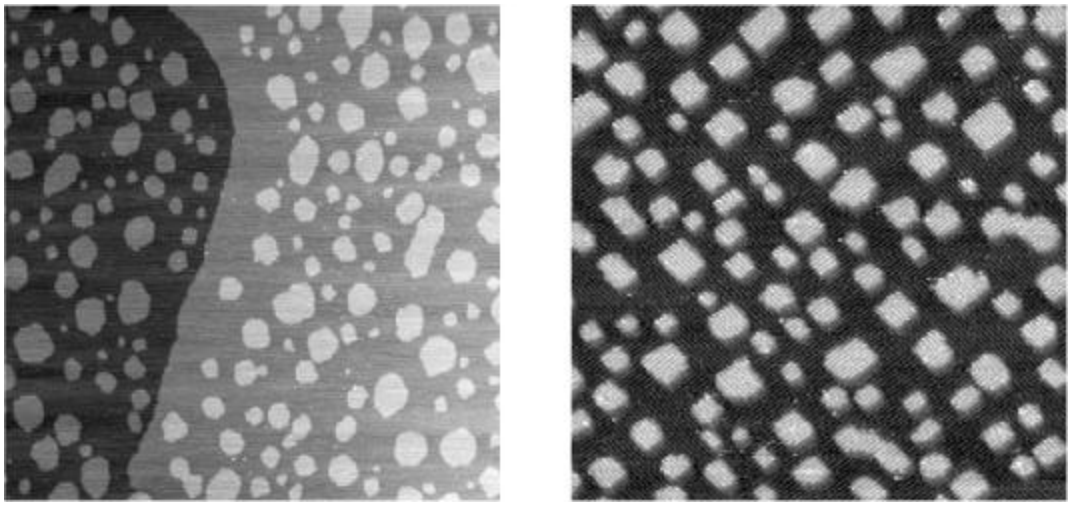

STM images of unreconstructed **Au(100)** surfaces in 0.1 M $H_2SO_4$. (a) E = 0.63 V vs. SCE. 400 x 400 $nm^2$. The image (b) was recorded at E = 0.35 V vs. SCE just after the lifting of the reconstruction and shows rows of adsorbed (bi)sulfate. Courtesy of M. Kleinert.

(a) (b)

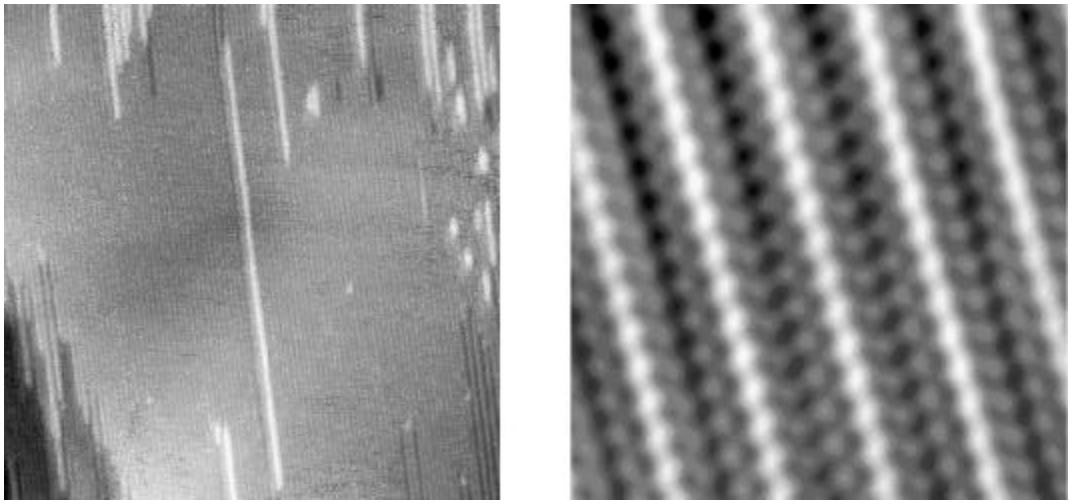

STM images of a reconstructed **Au(110)** electrode in 0.1 M $H_2SO_4$ at -0.2 V vs. SCE. (a) 80 x 80 $nm^2$. (b) High-resolution image of the (1x2) missing-row structure. 5 x 5 $nm^2$. Courtesy of M. Kleinert.

(a) (b)

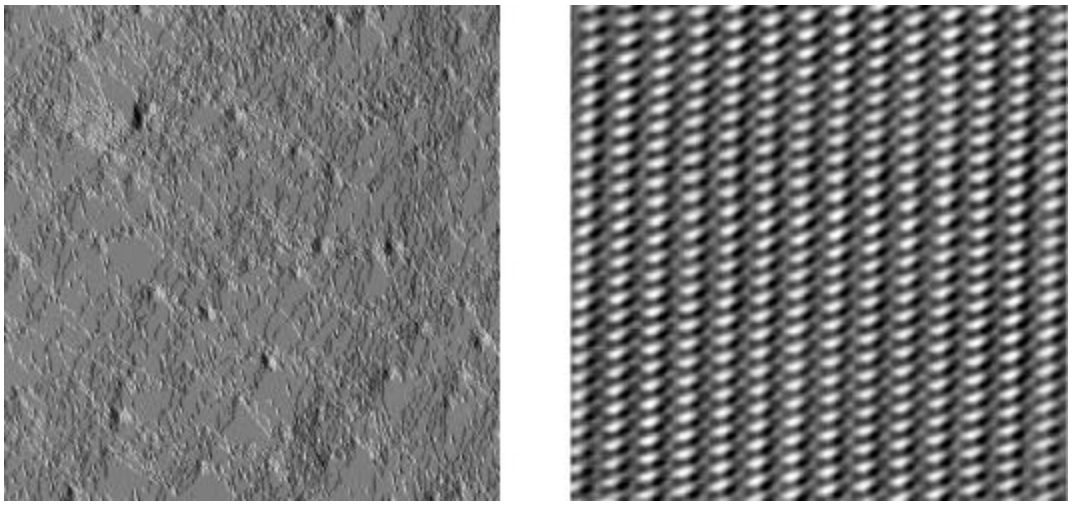

**Au(110)** electrodes in 0.1 M $H_2SO_4$. (a) STM image (500 x 500 $nm^2$) demonstrating the high density of surface defects and the difficulty in getting large well-ordered terraces. E = -0.05 V vs. SCE. (b) High-resolution image of the (1x1) structure at 0.35 V. 8 x 8 $nm^2$. Courtesy of M. Kleinert.

(a) (b)

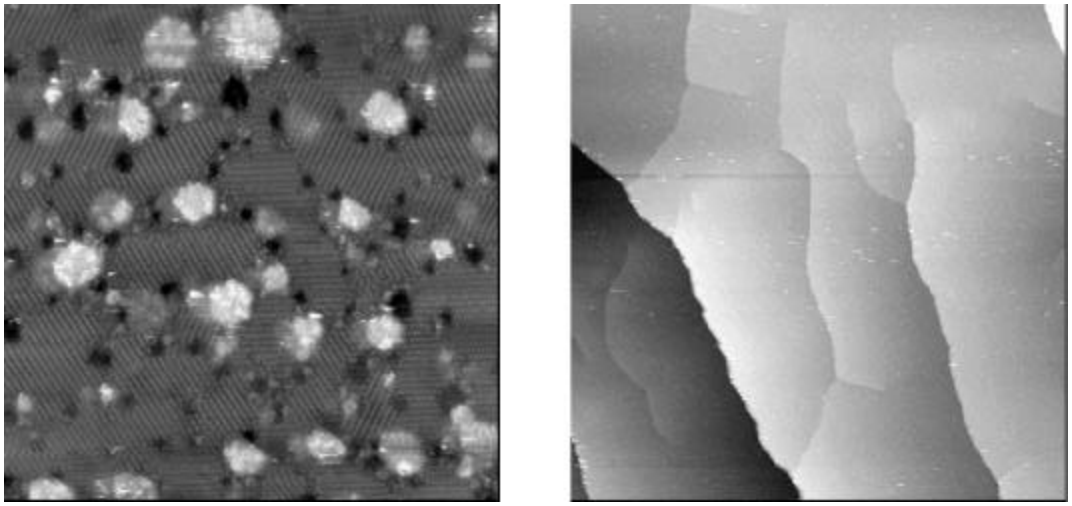

STM images of Pd single crystal surfaces in 0.1 M $H_2SO_4$ at E = 0.25 V vs. SCE. The electrodes were annealed by inductive heating in nitrogen and cooled in the same atmosphere [Cue00]. (a) Domains of the ( $\sqrt{3}$x$\sqrt{7}$ )R19.1° (bi)sulfate structure on **Pd(111)** (50 x 50 $nm^2$). (b) Large-scale image of **Pd(100)**, showing several screw dislocations (500 x 500 $nm^2$). Courtesy of A. Cuesta.

(a) (b)

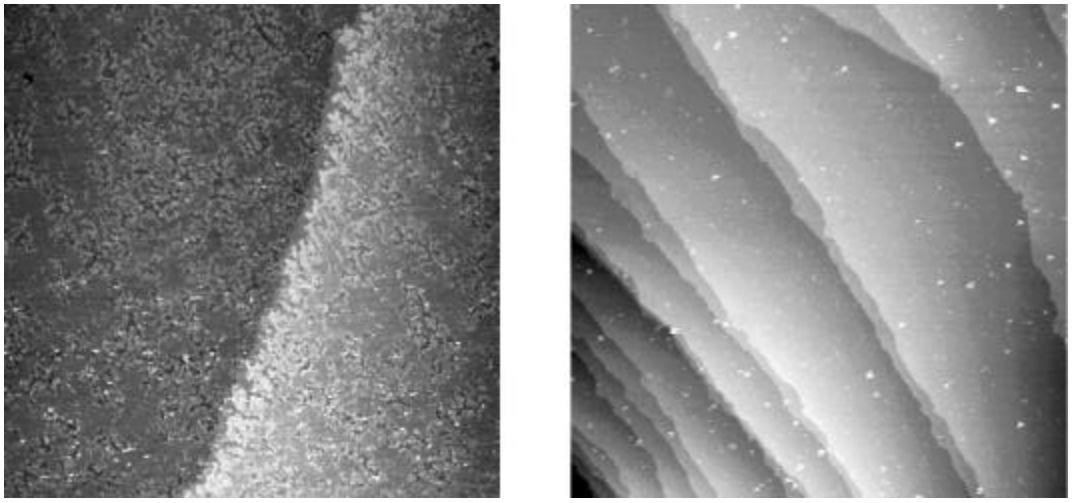

STM images of flame-annealed **Pt(111)** electrodes, cooled (a) in air and (b) in $N_2$ + CO. E = 0.35 V. 0.1 M $H_2SO_4$. 500 x 500 $nm^2$. Courtesy of M. Kleinert.

(a) (b)

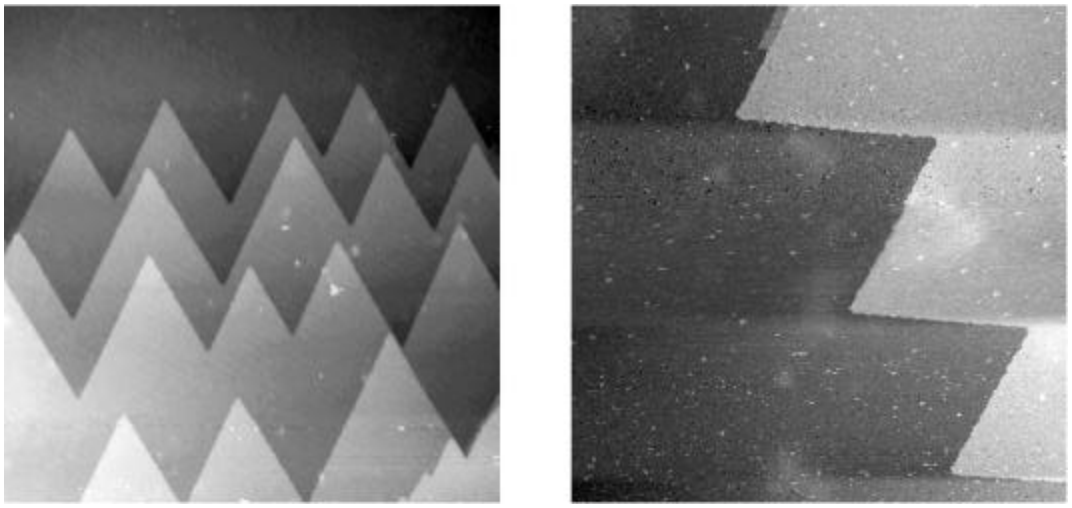

STM images at 0.35 V in 0.1 M $H_2SO_4$ of **Pt(111)** electrodes, prepared by flame-annealing and cooling under a strong $H_2$ stream. (a) 1000 x 1000 $nm^2$. (b) 500 x 500 $nm^2$. Courtesy of M. Kleinert.

(a) (b)

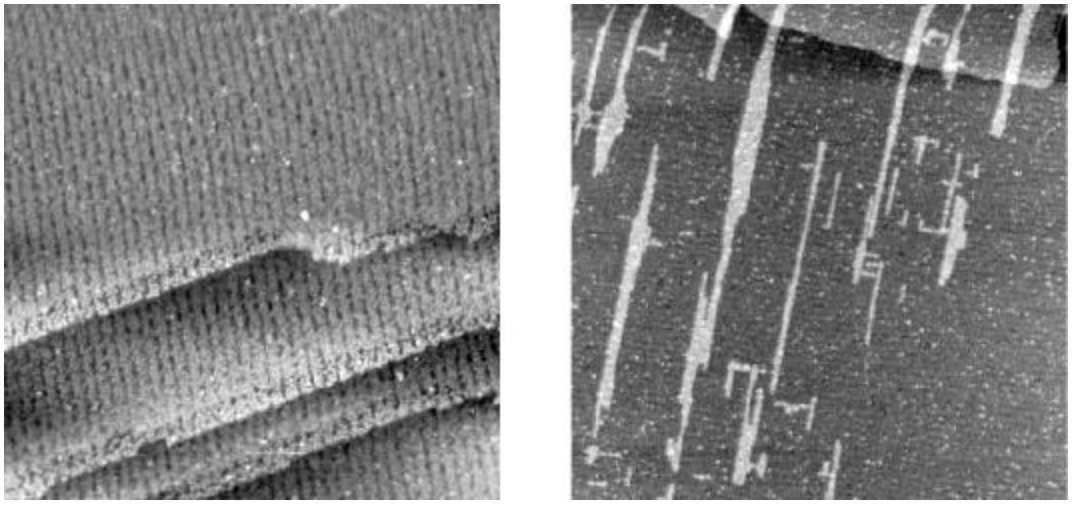

STM images of **Pt(100)** electrodes, prepared by flame-annealing and cooling in air. 0.1 M $H_2SO_4$. E = -0.15 V vs. SCE. (a) 150 x 150 $nm^2$. (b) 200 x 200 $nm^2$. Courtesy of M. Kleinert.

(a) (b)

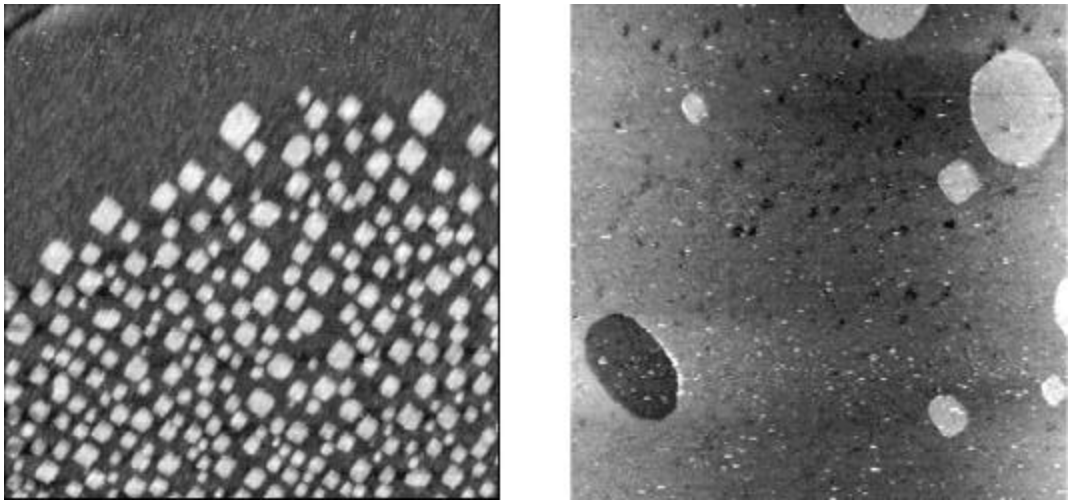

STM images of **Pt(100)** electrodes in 0.1 M $H_2SO_4$, prepared by flame-annealing and cooling (a) in $N_2$ + $H_2$. E = -0.15 V vs. SCE. 225 x 225 $nm^2$ and (b) under a strong $H_2$ stream. E = -0.15 V vs. SCE. 730 x 730 $nm^2$. Courtesy of M. Kleinert.

(a) (b)

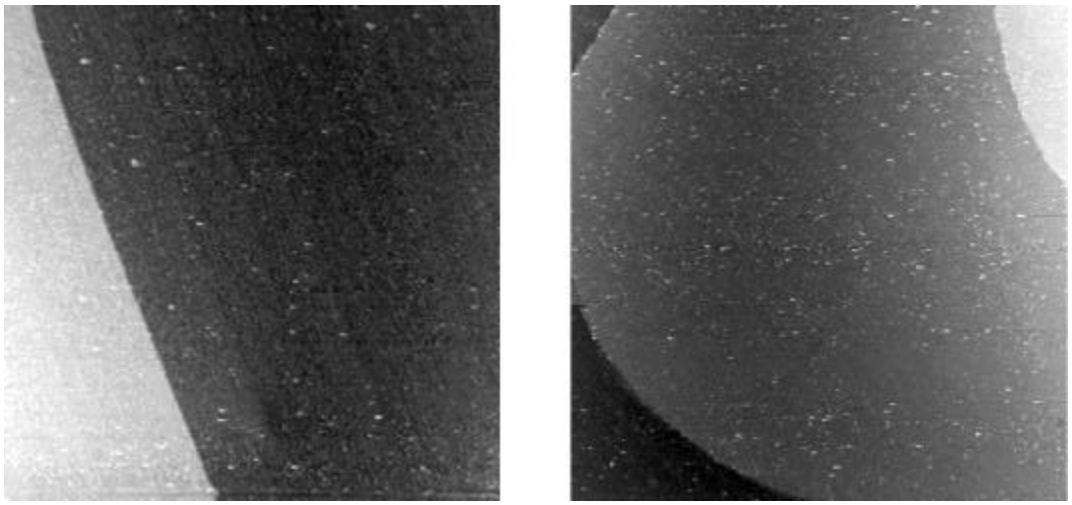

STM images of flame-annealed **Pt(100)** electrodes in 0.1 M $H_2SO_4$. (a) Cooling in $N_2$ leads to a flat and possibly reconstructed surface. E = 0.45 V vs. SCE. 314 x 314 $nm^2$. (b) After cooling in a $N_2$ + CO mixture, a flat and well-ordered unreconstructed surface is obtained. E = -0.15 V vs. SCE. 800 x 800 $nm^2$. Courtesy of M. Kleinert.

(a) (b)

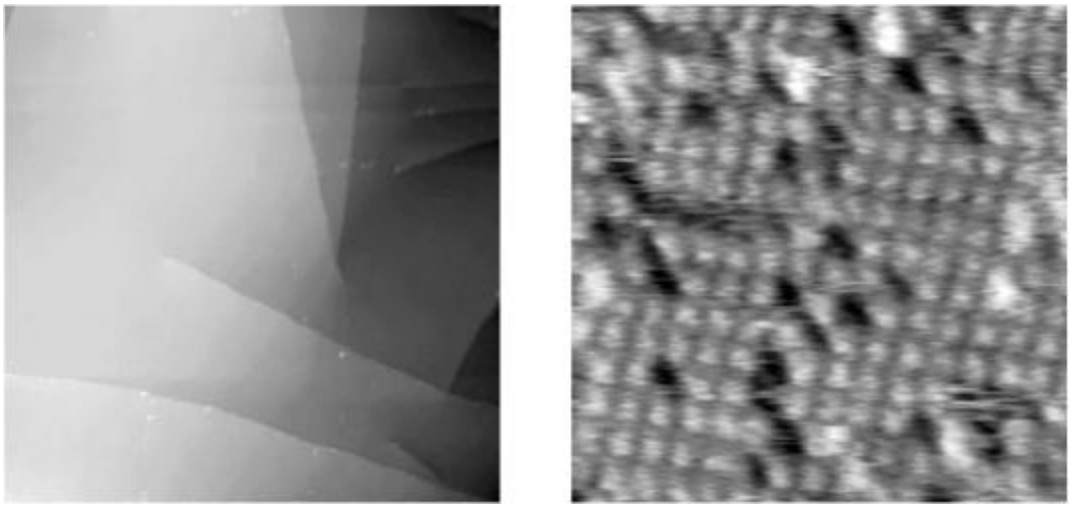

STM images of **Rh(111)** in air. (a) Atomically flat surface with screw dislocations after cooling in a CO atmosphere (750 x 750 $nm^2$). (b) High resolution image of an ordered CO adlayer (12 x 12 $nm^2$). Courtesy of M. Kleinert.

## 7. References


[Abe86] D. Aberdam, R. Durand, R. Faure, F. El-Omar
*Structural changes of a Pt(111) electrode induced by electrosorption of oxygen in acidic solutions: a coupled voltammetry, LEED and AES study*
Surf. Sci. 171 (1986) 303

[Akl99] A. Al-Akl, G.A. Attard, R. Price, B. Timothy
*Voltammetric and UHV charaterisation of the (1x1) and reconstructed hex-R0.7° phases of Pt{100}*
J. Electroanal. Chem. 467 (1999) 60

[Aziz02] A.M. El-Aziz, L.A. Kibler, D.M. Kolb
*The potentials of zero charge of Pd(111) and thin Pd overlayers on Au(111)*
Electrochem. Communications 4 (2002) 535

[Bal93] M. Baldauf, D.M. Kolb
*A hydrogen adsorption and absorption study with ultrathin Pd overlayers on Au(111) and Au(100)*
Electrochim. Acta 38 (1993) 2145

[Bal96] M. Baldauf, D.M. Kolb
*Formic acid oxidation on ultrathin Pd films on Au(hkl) and Pt(hkl)*
J. Phys. Chem. 100 (1996) 11375

[Bar90] J.V. Barth, H. Brune, G. Ertl, R.J. Behm
*Scanning tunneling microscopy observations on the reconstructed Au(111) surface: Atomic structure, long-range superstructure, rotational domains, and surface defects*
Phys. Rev. B 42 (1990) 9307

[Bat92] N. Batina, T. Will, D.M. Kolb
*Study of initial stages of copper deposition by in situ scanning tunneling microscopy*
Faraday Discuss. 94 (1992) 93

[Bat94] N. Batina, A.S. Dakkouri, D.M. Kolb
*The surface structure of flame-annealed Au(100) in aqueous solution: An STM study*
J. Electroanal. Chem. 370 (1994) 87

[Bat95] N. Batina, T. Yamada, K. Itaya
*Atomic level characterization of the iodine modified Au(111) electrode surface in perchloric acid solution by in-situ STM and ex-situ LEED*
Langmuir 11 (1995) 4568

[Bei95] G. Beitel, O.M. Magnussen, R.J. Behm
*Atomic structure of clean and Cu covered Pt(110) electrodes*
Surf. Sci. 336 (1995) 19

[Bew75] A. Bewick, B. Thomas
*Optical and electrochemical studies of the underpotential deposition of metals. Part I. Thallium deposition on single crystal silver electrodes*
J. Electroanal. Chem. 65 (1975) 911

[Bin83] G. Binnig, H. Rohrer, Ch. Gerber, E. Weibel
*(111) facets as the origin of reconstructed Au(110) surfaces*
Surf. Sci. 131 (1983) L379

[Bit96] A. Bittner
*Elektrochemische Rastertunnelmikroskopie der Halogenadsorption und Kupferabscheidung an Platin Einkristallen*
PhD Thesis, FU Berlin (1996)

[Bot93] M. Bott, M. Hohage, Th. Michely, G. Comsa
*Pt(111) reconstruction induced by enhanced Pt gas-phase chemical potential*
Phys. Rev. Lett. 70 (1993) 1489

[Bra01] S.R. Brankovic, J. McBreen, R.R. Adzic
*Spontaneous deposition of Pd on a Ru(0001) surface*
Surf. Sci. 479 (2001) L363

[Bra02] S.R. Brankovic, J.X. Wang, Y. Zhu, R. Sabatini, J. McBreen, R.R. Adzic
*Electrosorption and catalytic properties of bare and Pt modified single crystal and nanostructured Ru surfaces*
J. Electroanal. Chem. 524-525 (2002) 231.

[Bud66] E. Budewski, W. Bostanoff, T. Witanoff, Z. Stoinoff, A. Kotzewa, R. Kaischew
*Keimbildungserscheinungen an versetzungsfreien (100)-Flächen von Silbereinkristallen*
Electrochim. Acta 11 (1966) 1697

[Bud96] E. Budevski, G. Staikov, W.J. Lorenz
*Electrochemical phase formation and growth*
VCH, Weinheim (1996)

[Cao93] E.Y. Cao, D.A. Stern, J.Y. Gui, A.T. Hubbard
*Studies of Ru(001) electrodes in aqueous electrolytes containing silver ions and methane: LEED, HREELS, Auger spectroscopy and electrochemistry*
J. Electroanal. Chem. 354 (1993) 71.

[Cha86] C.-M. Chan, M.A. Van Hove
*Confirmation of the missing-row model with three-layer relaxations for the reconstructed Ir(110)-(1x2) surface*
Surf. Sci. 171 (1986) 226

[Chi88] T. Chierchie, C. Mayer
*Voltammetric study of the underpotential deposition of copper on polycrystalline and single crystal palladium surfaces*
Electrochim. Acta 33 (1988) 341

[Cla80a] J. Clavilier, R. Faure, G. Guinet, R. Durand
*Preparation of monocrystalline Pt microelectrodes and electrochemical study of the plane surfaces cut in the direction of the {111} and {110} planes*
J. Electroanal. Chem. 107 (1980) 205

[Cla80b] J. Clavilier
*The role of anion on the electrochemical behavoiur of a {111} platinum surface; an unusual splitting of the voltammogram in the hydrogen region*
J. Electroanal. Chem. 107 (1980) 211

[Cla86] J. Clavilier, D. Armand, S.G. Sun, M. Petit
*Electrochemical adsorption behaviour of platinum stepped surfaces in sulfuric acid solutions*
J. Electroanal. Chem. 205 (1986) 267

[Cla89] J. Clavilier, J.M. Feliu, A. Fernandez-Vega, A. Aldaz
*Electrochemical behaviour of irreversibly adsorbed bismuth on Pt(100) with different degrees of crystalline surface order*
J. Electroanal. Chem. 269 (1989) 175

[Cla91] J. Clavilier, A. Rodes, K. El Achi, M.A. Zamakhchari
*Electrochemistry at platinum single crystal surfaces in acidic media: hydrogen and oxygen adsorption*
J. Chim. Phys. 88 (1991) 1291

[Cla94a] J. Clavilier, M. Wasberg, M. Petit, L.H. Klein
*Detailed analysis of the voltammetry of Rh(111) in perchloric acid solution*
J. Electroanal. Chem. 374 (1994) 123

[Cla94b] J. Clavilier, J.M. Orts, J.M. Feliu
*Etude de l´effet de prétraitements sur la topographie des surfaces orientées de platine par deux méthodes indépendantes : voltammétrie et STM*
J. Phys. IV 4 (1994) 303

[Cla99] J. Clavilier
*Flame-annealing and cleaning technique*
in: Interfacial Electrochemistry: Theory, Experiment, and Applications
A. Wieckowski (ed.), M. Dekker, New York, p. 231

[Cue99] A. Cuesta, L.A. Kibler, D.M. Kolb
*A method to prepare single crystal electrodes of reactive metals: application to Pd(hkl)*
J. Electroanal. Chem. 466 (1999) 165

[Cue00] A. Cuesta
unpublished results

[Dal99] L.H. Dall`Antonia, J. Perez, G. Tremiliosi-Filho, E.R. Gonzalez
*Metodologia para o cerscimento de esferas monocristalinas de metais nobres*
Química nova 22 (1999) 760

[Dak96] A.S. Dakkouri
*Untersuchungen zur Rekonstruktion von und Adsorption organischer Moleküle auf Au(100)- und Au(111)-Elektroden mit Hilfe der in situ Rastertunnelmikroskopie*
PhD Thesis, University of Ulm (1996)

[Dak97] A.S. Dakkouri
*Reconstruction phenomena at gold/electrolyte interfaces: an in-situ STM study of Au(100)*
Solid State Ionics 94 (1997) 99

[Dak99] A.S. Dakkouri, D.M. Kolb
*Reconstruction of gold surfaces*
in: Interfacial Electrochemistry: Theory, Experiment, and Applications
A. Wieckowski (ed.), M. Dekker, New York, p. 151

[Dic76] D. Dickertmann, F.D. Koppitz, J.W. Schultze
*Eine Methode zum Ausschluss von Randeffekten bei elektrochemischen Messungen an Einkristallen*
Electrochim. Acta 21 (1976) 967

[Die96] M. Dietterle
*Untersuchungen zur elektrolytischen Cu-Abscheidung und zur Dynamik von Stufenkanten auf niedrigindizierten Ag-Elektroden: Eine in-situ STM Studie*
PhD Thesis, University of Ulm (1996)

[Dis98] M.H. Dishner, M.M. Ivey, S. Gorer, J.C. Hemminger, F.J. Feher
*Preparation of gold thin films by epitaxial growth on mica and the effect of flame annealing*
J. Vac. Sci. Technol. A 16 (1998) 3295

[Dre97] Th. Dretschkow, Th. Wandlowski
*The kinetics of structural changes in anionic adlayers on stepped Au(111)$_s$ electrodes from sulfuric acid solutions*
Ber. Bunsenges. Phys. Chem. 101 (1997) 749

[Dwe73] A.W. Dweydari, C.H.B. Mee
*Oxygen adsorption on the (111) face of silver*
Phys. Status Solidi A 17 (1973) 247

[Dwe75] A.W. Dweydari, C.H.B. Mee
*Work function measurements on (100) and (110) surfaces of silver*
Phys. Status Solidi A 27 (1975) 223

[Ebe00] D. Eberhardt
unpublished results

[Ede94] G.J. Edens, X. Gao, M.J. Weaver
*The adsorption of sulfate on gold(111) in acidic aqueous media: adlayer structural inferences from infrared spectroscopy and scanning tunneling microscopy*
J. Electroanal. Chem. 375 (1994) 357

[Fed67] D.G. Fedak, N.A. Gjostein
*On the anomalous surface structures of gold*
Surf. Sci. 8 (1967) 77

[Fel94a] J.M. Feliu, J.M. Orts, R. Gómez, A. Aldaz, J. Clavilier
*New information on the unusual adsorption states of Pt(111) in sulfuric acid solutions from potentiostatic adsorbate replacement by CO*
J. Electroanal. Chem. 372 (1994) 265

[Fel94b] J.M. Feliu, A. Rodes, J.M. Orts, J. Clavilier
*The problem of surface order of Pt single crystals in electrochemistry*
Pol. J. Chem. 68 (1994) 1575

[Fun95] A.M. Funtikov, U. Linke, U. Stimming, R. Vogel
*An in-situ STM study of anion adsorption on Pt(111) from sulfuric acid solutions*
Surf. Sci. 324 (1995) L343

[Fun97] A.M. Funtikov, U. Stimming, R. Vogel
*Anion adsorption from sulfuric acid solutions on Pt(111) single crystal electrodes*
J. Electroanal. Chem. 428 (1997) 147

[Gao91a] X. Gao, A. Hamelin, M.J. Weaver
*Potential-dependent reconstruction at ordered Au(100)-aqueous interfaces as probed by atomic-resolution scanning tunneling microscopy*
Phys. Rev. Lett. 67 (1991) 618

[Gao91b] X. Gao, A. Hamelin, M.J. Weaver
*Reconstruction at ordered Au(110)-aqueous interfaces as probed by atomic-resolution scanning tunneling microscopy*
Phys. Rev. B 44 (1991) 10983

[Gao92] X. Gao, A. Hamelin, M.J. Weaver
*Elucidating complex surface reconstructions with atomic-resolution scanning tunneling microscopy: Au(100)-aqueous electrochemical interface*
Phys. Rev. B 46 (1992) 7096

[Góm93] R. Gómez, J. Clavilier
*Electrochemical behaviour of platinum surfaces containing (110) sites and the problem of the third oxidation peak*
J. Electroanal. Chem. 354 (1993) 189

[Góm97] R. Gómez, J.M. Orts, J.M. Feliu, J. Clavilier, L.H. Klein
*The role of surface crystalline heterogeneities in the electrooxidation of carbon monoxide adsorbed on Rh(111) electrodes in sulfuric acid solutions*
J. Electroanal. Chem. 432 (1997) 1

[Gun91] H.-J. Guntherodt and R. Wiesendanger (Eds.), in Scanning Tunneling Microscopy I, Springer-Verlag, Berlin, 1991

[Hai91] W. Haiss, D. Lackey, J.K. Sass, K.H. Besocke
*Atomic resolution scanning tunneling microscopy images of Au(111) surfaces in air and polar organic solvents*
J. Chem. Phys. 95 (1991) 2193

[Ham85] A. Hamelin
*Double-layer properties at sp and sd metal single-crystal electrodes*
Modern Aspects of Electrochemistry, No. 16, B.E. Conway, R.E. White, J.O`M. Bockris (Eds.), Plenum Press, New York (1985) p. 1

[Ham87a] A. Hamelin, L. Doubova, D. Wagner, H. Schirmer
*A modification of the last step of surface preparation for gold and silver single crystal faces*
J. Electroanal. Chem. 220 (1987) 155

[Ham87b] A. Hamelin, L. Stoicoviciu
*Study of gold low index faces in $KPF_6$ solutions. Part I. Experimental behaviour and determination of the points of zero charge*
J. Electroanal. Chem. 234 (1987) 93

[Ham96] A. Hamelin
*Cyclic voltammetry at gold single-crystal surfaces. Part 1. Behaviour at low-index faces*
J. Electroanal. Chem. 407 (1996) 1

[Han78] G.V. Hansson, S.A. Flodström
*Photoemission study of the bulk and surface electronic structure of single crystals of gold*
Phys. Rev. B 18 (1978) 1572

[Höl95] M.H.F. Hölzle
*Zweidimensionale Phasenübergänge in adsorbierten Monoschichten*
PhD Thesis, University of Ulm (1995)

[Höl95a] M.H. Hölzle, V. Zwing, D.M. Kolb
*The influence of steps on the deposition of Cu on Au(111)*
Electrochim. Acta 40 (1995) 1237

[Hor99] S. Horch, H.T. Lorensen, S. Helveg, E. Lægsgaard, I. Stensgaard, K.W. Jacobsen, J.K. Nørskov, F. Besenbacher
*Enhancement of surface self-diffusion of platinum atoms by adsorbed hydrogen*
Nature 398 (1999) 134

[Hos97] N. Hoshi, M. Noma, T. Suzuki, Y. Hori
*Structural effect on the rate of $CO_2$ reduction on single crystal electrodes of palladium,* J. Electroanal. Chem. 421 (1997) 15

[Hos00] N. Hoshi, K. Kagaya, Y. Hori
*Voltammograms of the single-crystal electrodes of palladium in aqueous sulfuric acid electrolyte: Pd(S)-[n(111)x(111)] and Pd(S)-[n(100)x(111)]*
J. Electroanal. Chem. 485 (2000) 55

[Hos02] N. Hoshi, M. Kuroda, Y. Hori
*Voltammograms of stepped and kinked stepped surfaces of palladium: Pd(S)-[n(111)x(100)] and Pd(S)-[n(100)x(110)]*
J. Electroanal. Chem. 521 (2002) 155

[Hou87] M. Hourani, A. Wieckowski
*Electrochemistry of the ordered Rh(111) electrode. Surface preparation and voltammetry in $HClO_4$ electrolyte*
J. Electroanal. Chem. 227 (1987) 259

[Hov81] M.A. Van Hove, R.J. Koestner, P.C. Stair, J.P. Bibérian, L.L. Kesmodel, I. Bartos, G.A. Somorjai
*The surface reconstructions of the (100) crystal faces of iridium, platinum and gold.*
*I. Experimental observations and possible structural models*
Surf. Sci. 103 (1981) 189
*II. Structural determination by LEED intensity analysis*
Surf. Sci. 103 (1981) 218

[Hub88] A.T. Hubbard
*Electrochemistry at well-characterized surfaces*
Chem. Rev. 88 (1988) 633

[Ita90] K. Itaya, S. Sugawara, K. Sashikata, N. Furuya
*In situ scanning tunneling microscopy of platinum (111) surface with the observation of monoatomic steps*
J. Vac. Sci. Technol. 8 (1990) 515

[Ita98] K. Itaya
*In situ scanning tunneling microscopy in electrolyte solutions*
Prog. Surf. Sci. 58 (1998) 121

[Ita99] K. Itaya
*Atomic-scale aspects of anodic dissolution of metals: studies by in situ scanning tunneling microscopy*
in: Interfacial Electrochemistry: Theory, Experiment, and Applications
A. Wieckowski (ed.), M. Dekker, New York, p. 187

[Kib99] L.A. Kibler, M. Kleinert, D.M. Kolb
*The initial stages of rhodium deposition on Au(111)*
J. Electroanal. Chem. 467 (1999) 249

[Kib00] L.A. Kibler, *Elektrochemie an wohldefinierten Edelmetalloberflächen: Struktur und katalytische Eigenschaften dünner Palladium- und Rhodiumschichten auf Gold- und Platineinkristallektroden*
PhD Thesis, University of Ulm (2000)

[Kib00a] L.A. Kibler, A. Cuesta, M. Kleinert, D.M. Kolb
*In-situ characterisation of the surface morphology of platinum single crystal electrodes as a function of their preparation*
J. Electroanal. Chem. 484 (2000) 73

[Kib02] A.M. El-Aziz, L.A. Kibler
*Influence of steps on the electrochemical oxidation of CO adlayers on Pd(111) and on Pd films electrodeposited onto Au(111)*
J. Electroanal. Chem. 535 (2002) 107.

[Kib02b] A.M. El-Aziz, L.A. Kibler
*New information about the electrochemical behaviour of Ru(0001) in perchloric acid solutions*
Electrochem. Comm. 4 (2002) 866.

[Kit89] C. Kittel
*Einführung in die Festkörperphysik*
Oldenbourg, München (1989)

[Kle99] M. Kleinert, A. Cuesta, L.A. Kibler, D.M. Kolb
*In-situ observation of an ordered sulfate adlayer on Au(100)*
Surf. Sci. 430 (1999) L521

[Kle00] M. Kleinert
unpublished results

[Kol86] D.M. Kolb, J. Schneider
*Surface reconstruction in electrochemistry: Au(100)-(5x20), Au(111)-(1x23) and Au(110)-(1x2)*
Electrochim. Acta 31 (1986) 929

[Kol96] D.M. Kolb
*Reconstruction phenomena at metal-electrolyte interfaces*
Prog. Surf. Sci. 51 (1996) 109

[Lan83] E. Lang, K. Müller, K. Heinz, M.A. Van Hove, R.J. Koestner, G.A. Somorjai
*LEED intensity analysis of the (1x5) reconstruction of Ir(100)*
Surf. Sci. 127 (1983) 347

[Lec78] J. Lecoeur, C. Sella, J.-C. Martin, M.J.-J. Trillat
*Etude des courbes capacité différentielle - potentiel, dans le cas d` électrodes d´ or (100) massives ou en couches minces, au contact de solutions aqueuses de fluorure de sodium*
C.R. Acad. Sc. Paris C 287 (1978) 447

[Lec90] J. Lecoeur, J.P. Bellier, C. Koehler
*Comparison of crystallographic anisotropy effects on potential of zero charge and electronic work function for gold {111}, {311}, {110} and {210} orientations*
Electrochim. Acta 35 (1990) 1383

[Lee02] J. Lee, W.B. Wang, M.S. Zei, G.Ertl
*Electrocatalytic oxidation of CO on Ru(0001) surfaces: The influence of surface disorder*
Phys. Chem. Chem. Phys. 4 (2002) 1393

[Leu89] L.W.H. Leung, S.C. Chang, M.J. Weaver
*Electrochemical infrared spectoscopy of carbon monoxide on ordered rhodium (111): Comparison with vibrational spectra on Pt(111) and in related surface-vacuum environments*
J. Chem. Phys. 90 (1989) 7426

[Lin00] W.F. Lin, M.S. Zei, Y.D. Kim, H. Over, G. Ertl
*Electrochemical versus Gas-Phase Oxidation of Ru Single-Crystal Surfaces*
J. Phys. Chem. B 104 (2000) 6040

[Lin00b] W.F. Lin, P.A. Christensen, A. Hamnett, M.S. Zei, G. Ertl
*The Electro-Oxidation of CO at the Ru(0001) Single-Crystal Electrode Surface*
J. Phys. Chem. B 104 (2000) 6642

[Liu91] C.L. Liu, J.M. Cohen, J.B. Adams, A.F. Voter
EAM study of surface self-diffusion of single adatoms of fcc metals Ni, Cu, Al, Ag, Au, Pd, and Pt
Surf. Sci. 253 (1991) 334

[Llo93] M.J. Llorca, J.M. Feliu, A. Aldaz, J. Clavilier
*Electrochemical structure-sensitive behaviour of irreversibly adsorbed palladium on Pt(100), Pt(111) and Pt(110) in an acidic medium*
J. Electroanal. Chem. 351 (1993) 299

[Lu02] P.-C. Lu, C.-H. Yang, S.-L. Yau, M.-S. Zei
*In situ scanning tunneling microscopy of (bi)sulfate, oxygen, and iodine adlayers chemisorbed on a well-defined Ru(001) electrode prepared in a non-ultrahigh-vacuum environment*
Langmuir 18 (2002) 754.

[Luc97] C.A. Lucas, N.M. Markovic, P.N. Ross
*Electrochemical deposition of copper onto Pt(111) in the presence of (bi)sulfate anions*
Phys. Rev. B 56 (1997) 3651

[Mag92] O.M. Magnussen, J. Hageböck, J. Hotlos, R.J. Behm
*In-situ STM observations of a disorder-order phase transition in bisulfate adlayers on Au(111)*
Faraday Discuss. 94 (1992) 329

[Mag93a] O.M. Magnussen, J. Wiechers, R.J. Behm
*In situ scanning tunneling microscopy observations of the potential-dependent (1x2) reconstruction on Au(110) in acidic electrolytes*
Surf. Sci. 289 (1993) 139

[Mag93b] O.M. Magnussen, J. Hotlos, R.J. Behm, N. Batina, and D.M. Kolb
*An in-situ scanning tunneling microscopy study of electrochemically induced "hex" « (1x1) transitions on Au(100) electrodes*
Surf. Sci. 296 (1993) 310

[Mar83] L.D. Marks
*Direct imaging of carbon-covered and clean gold(110) surfaces*
Phys. Rev. Lett. 51 (1983) 1000

[Mar86] N.M. Markovic, M. Hanson, G. McGougall, E. Yeager
*The effects of anions on hydrogen electrosorption on platinum single-crystal electrodes*
J. Electroanal. Chem. 214 (1986) 555

[Mar97] N.M. Makovic, B.N. Grgur, C.A. Lucas, P.N. Ross
*Surface electrochemistry of CO on Pt(110)-(1x2) and Pt(110)-(1x1) surfaces*
Surf. Sci. 384 (1997) L805

[Mar00] N.S. Marinkovic, J.X. Wang, H. Zajonz, R.R. Adzic
*Unusual Stability of Carbon Monoxide Adsorbed on the Ru(0001) Electrode Surface*
Electrochem. Solid State Lett. 3 (2000) 508

[Mar01] N.S. Marinkovic, J.X. Wang, H. Zajonz, R.R. Adzic
*Adsorption of bisulfate on the Ru(0001) single crystal electrode surface*
J. Electroanal. Chem. 500 (2001) 388.

[Mat00] http://www.mateck.de

[Mic91] T. Michely, G. Comsa
*Temperature dependence of the sputtering morphology of Pt(111)*
Surf. Sci. 256 (1991) 217

[Mic92] R. Michaelis, M.S. Zei, R.S. Zhai, D.M. Kolb
*The effect of halides on the structure of Cu UPD onto Pt(111): A LEED and ESCA study*
J. Electroanal. Chem. 339 (1992) 299

[Mor85] W. Moritz, D. Wolf
*Multilayer distortion in the reconstructed (110) surface of Au*
Surf. Sci. 163 (1985) L655

[Möl86] J. Möller, H. Niehus, W. Heiland
*Direct measurement of Au(110) surface structural parameters by low energy ion backscattering*
Surf. Sci. 166 (1986) L111

[Mot84a] S. Motoo, N. Furuya
*Hydrogen and oxygen adsorption on Ir(111), Ir(100) and Ir (110) planes*
J. Electroanal. Chem. 167 (1984) 309

[Mot84b] S. Motoo, N. Furuya
*Effect of anions on hydrogen and oxygen adsorption on iridium single crystal surfaces*
J. Electroanal. Chem. 181 (1984) 301

[Mot84c] S. Motoo, N. Furuya
*Electrochemistry of platinum single crystal surfaces. Part I. Structural change of the Pt(111) surface followed by an electrochemical method*
J. Electroanal. Chem. 172 (1984) 339

[Mot87] S. Motoo, N. Furuya
*Effect of terraces and steps in the electrocatalysis for formic acid oxidation on platinum*
Ber. Bunsenges. Phys. Chem. 91 (1987) 457

[Oka01] J. Okada, J. Inukai, K. Itaya
*Underpotential and bulk deposition of copper on Pd(111) in sulfuric acid solution studied by in situ scanning tunneling microscopy*
Phys. Chem. Chem. Phys. 3 (2001) 3297

[Pot75] H.C. Potter, J.M. Blakeley
*LEED, Auger spectroscopy, and contact potential studies of copper-gold alloy single crystal surfaces*
J. Vac. Sci. Technol. 12 (1975) 635

[Pre73] E. Preuss, B. Krahl-Urban, R. Butz
*Laue Atlas*
Bertelsmann Universitätsverlag (1973)

[Rav90] R. Raval, S. Haq, M.A. Harrison, G. Blyholder, D.A. King
*Molecular adsorbate-induced surface reconstruction: CO/Pd(110)*
Chem. Phys. Lett. 167 (1990) 391

[Rhe90] C.K. Rhee, M. Wasberg, G. Horanyi, A. Wieckowski
*Strong anion/surface interactions: perchlorate reduction on Rh(100) electrode studied by voltammetry*
J. Electroanal. Chem. 291 (1990) 281

[Rob92] K.M. Robinson, I.K. Robinson, W.E. O`Grady
*Structure of Au(100) and Au(111) single crystals surfaces prepared by flame annealing*
Surf. Sci. 262 (1992) 387

[Rob84] I.K. Robinson, Y. Kuk, L.C. Feldman
*Domain structure of the clean reconstructed Au(110) surface*
Phys. Rev. B 29 (1984) 4762

[Rob95] K.M. Robinson, W.E. O`Grady
*X-ray diffraction and electrochemical study on the oxidation of flame-annealed Au(100) single-crystal surfaces*
J. Electroanal. Chem. 384 (1995) 139

[Rom93] U. Romahn, P. von Blanckenhagen, C. Kroll, W. Göpel
*Step-induced deconstruction and step-height evolution of the Au(110) surface*
Phys. Rev. B 47 (1993) 12840

[Ros84] P.N. Ross, F.T. Wagner
*The application of surface physics techniques to the study of electrochemical systems*
in: Advances in electrochemistry and electrochemical engineering, vol. 13, H. Gerischer, Ch.W. Tobias (eds.), Wiley-Interscience, New York (1984) p. 69

[San92] A.R. Sandy, S.G.J. Mochrie, D.M. Zehner, G. Grübel, K.G. Huang, D. Gibbs
*Reconstruction of the Pt(111) surface*
Phys. Rev. Lett. 68 (1992) 2192

[Sas91a] K. Sashikata, N. Furuya, K. Itaya
*In situ electrochemical scanning tunneling microscopy of single-crystal surfaces of Pt(111), Rh(111), and Pd(111) in aqueous sulfuric acid solution*
J. Vac. Sci. Technol. B9 (1991) 457

[Sas91b] K. Sashikata, N. Furuya, K. Itaya
*In situ scanning tunneling microscopy of underpotential deposition of copper on platinum(111) in sulfuric acid solutions*
J. Electroanal. Chem. 316 (1991) 361

[Sas96] K. Sashikata, Y. Matsui, K. Itaya, M.P. Soriaga
*Adsorbed-iodine-catalyzed dissolution of Pd single-crystal electrodes: studies by electrochemical scanning tunneling microscopy*
J. Phys. Chem. 100 (1996) 20027

[Sas98] K. Sashikata, T. Sugata, M. Sugimasa, K. Itaya
*In situ scanning tunneling microscopy observation of a porphyrin adlayer on an iodine-modified Pt(100) electrode*
Langmuir 14 (1998) 2896

[Sch84] D.A. Scherson, D.M. Kolb
*Voltammetric curves for Au(111) in acid media: a comparison with Pt(111) surfaces*
J. Electroanal. Chem. 176 (1984) 353

[Sch75] T. Schober, V. Sorajic, A. Meisenberg
*On electropolishing palladium for transmission electron microscopy (TEM)*
Metallography 8 (1975) 259

[Sch94] J.H. Schott, H.S. White
*Halogen adlayers on Ag(111)*
J. Phys. Chem. 98 (1994) 291

[Schw02] M. Schweizer, D.M. Kolb
*First observation of an ordered sulfate adlayer on Ag single crystal electrodes*
Surf. Sci. 544 (2003) 93

[Sil90] A.F. Silva, M.J. Sottomayor, A. Hamelin
*The temperature coefficient of the potential of zero charge of the gold single-crystal electrode / aqueous solution interface. Possible relevance to gold-water interaction,* J. Electroanal. Chem. 294 (1990) 239

[Smo41] R. Smoluchowski
*Anisotropy of the electronic work function of metals*
Phys. Rev. 60 (1941) 661

[Som94] G.A. Somorjai
*Introduction to surface chemistry and catalysis*
Wiley-Interscience, New York (1994)

[Son86] R. Sonnenfeld, P.K. Hansma
*Atomic-resolution microscopy in water*
Science 232 (1986) 211

[Sor92] M.P. Soriaga
*UHV techniques in the study of electrode surfaces*
Prog. Surf. Sci. 39 (1992) 325

[Sou90] Southhampton Electrochemistry Group
*Instrumental Methods in Electrochemistry*
Ellis Horwood Series in Physical Chemistry, Ellis Horwood, London (1990)

[Sun95] Y.-E. Sung, S. Thomas, A. Wieckowski
*Characterization of the Rh(111) electrode by CEELS, AES, LEED, and voltammetry. Adsorption of (bi)sulfate, perchlorate, and carbon monoxide*
J. Phys. Chem. 99 (1995) 13513

[Sun99] S.-G. Sun, W.-B. Cai, L.-J. Wan, M. Osawa
*Infrared absorption enhancement for CO adsorbed on Au films in perchloric acid solutions and effects of surface structure studied by cyclic voltammetry, scanning tunneling microscopy and surface-enhanced IR spectroscopy*
J. Phys. Chem. B 103 (1999) 2460

[Str98] H. Striegler
*Rekonstruierte Elektrodenoberflächen im Kontakt mit organischen Verbindungen: Adsorption von Campher an Au(111) und Au(100)*
PhD Thesis, University of Ulm (1998)

[Stu96] M. Sturmat, R. Koch, K.H. Rieder
*Real Space Investigation of the Roughening and Deconstruction Transitions of Au(110)*
Phys. Rev. Lett. 77 (1996) 5071

[Tan95a] S. Tanaka, S.L. Yau, K. Itaya
*In-situ scanning tunneling microscopy of bromine adlayers on Pt(111)*
J. Electroanal. Chem. 396 (1995) 125

[Tan95b] H. Tanaka, J. Yoshinobu, M. Kawai
*Oxygen-induced reconstruction of the Pd(110) surface: an STM study*
Surf. Sci. 327 (1995) L505

[Teg56] W.J. McG Tegart
*The electrolytic and chemical polishing of metals in research and industry*
Pergamon, London (1956)

[Tit96] S. Titmuss, A. Wander, D.A. King
*Reconstruction of clean and adsorbate-covered metal surfaces*
Chem. Rev. 96 (1996) 1291

[Tra86] S. Trasatti, in Trends in Interfacial Electrochemistry, A.F. Silva (ed.)
*Potentials of zero charge, what they suggest about the structure of the interfacial region*
D. Reidel Publishing Company, Dordrecht (1986)

[TW95] T. Wandlowski
*Phase transitions in uracil adlayers on Ag, Au and Hg electrodes - substrate effects*
J. Electroanal. Chem. 395 (1995) 83

[Uch91] Y. Uchida, G. Lehmpfuhl
*Estimation of ad-vacancy formation energy on the Pt(111) surface by using reflection electron microscopy*
Surf. Sci. 243 (1991) 193

[Val81] G. Valette
*Double layer on silver single-crystal electrodes in contact with electrolytes having anions which present a slight specific adsorption. Part I. The (110) face*
J. Electroanal. Chem. 122 (1981) 285

[Val82a] G. Valette
*Double layer on silver single crystal electrodes in contact with electrolytes having anions which are slightly specifically adsorbed. Part II. The (100) face*
J. Electroanal. Chem. 138 (1982) 37

[Val82b] G. Valette
*Hydrophilicity of metal surfaces. Silver, gold and copper electrodes*
J. Electroanal. Chem. 139 (1982) 285

[Val89] G. Valette
*Double layer on silver single crystal electrodes in contact with electrolytes having anions which are slightly specifically adsorbed. Part III. The (111) face*
J. Electroanal. Chem. 269 (1989) 191

[Vli90] E. Vlieg, I.K. Robinson, K. Kern
*Relaxations in the missing-row structure of the (1x2) reconstructed surfaces of Au(110) and Pt(110)*
Surf. Sci. 233 (1990) 248

[Wag83] F.T. Wagner, P.N. Ross
*LEED analysis of electrode surfaces. Structural effects of potentiodynamic cycling on Pt single crystals*
J. Electroanal. Chem. 150 (1983) 141

[Wan95a] L.-J. Wan, S.-L. Yau, G.M. Swain, K. Itaya
*In-situ scanning tunneling microscopy of well-ordered Rh(111) electrodes*
J. Electroanal. Chem. 381 (1995) 105

[Wan95b] L.-J. Wan, S.-L. Yau, K. Itaya
*Atomic structure of adsorbed sulfate on Rh(111) in sulfuric acid solution*
J. Phys. Chem. 99 (1995) 9507

[Wan97] L.-J. Wan, S.-L. Yau, K. Itaya
*Structure of thiocyanate adlayers on Rh(111): an in situ STM study*
J. Solid State Electrochem. 1 (1997) 45

[Wan99] L.-J. Wan, M. Hara, J. Inukai, K. Itaya
*In situ scanning tunneling microscopy of well-defined Ir(111) surface: High-resolution imaging of adsorbed sulfate*
J. Phys. Chem. 103 (1999) 6978

[Wan00] L.-J. Wan, T. Suzuki, K. Sashikata, J. Okada, J. Inukai, K. Itaya
*In situ scanning tunneling microscopy of adsorbed sulfate on well-defined Pd(111) in sulfuric acid solution*
J. Electroanal. Chem. 484 (2000) 189

[Wan01] W.B. Wang, M.S. Zei, G. Ertl
*Electrosorption and electrooxidation of CO on Ru(0001)*
Phys. Chem. Chem. Phys. 3 (2001) 3307

[Wan02] W.B. Wang, M.S. Zei, G. Ertl
*Electrooxidation of CO on Ru(0001) and $RuO_2$(100) electrode surfaces*
Chem. Phys. Lett. 355 (2002) 301

[Wang01] J.X. Wang, N.S. Marinkovic, H. Zajonz, B.M. Ocko, R.R. Adzic
*In Situ X-Ray Reflectivity and Voltammetry Study of Ru(0001) Surface Oxidation in Electrolyte Solutions*
J. Phys. Chem. B 105 (2001) 2809.

[Wil88] K.-Th. Wilke, J. Bohm
*Kristallzüchtung*
VEB Verlag der Wissenschaften, Berlin (1988)

[Wu98] K. Wu, M.S. Zei
*Electrochemical behavior and structural changes of a reconstructed Pt(100) electrode in sulfuric acid: a comparison with Pt(100)-(1x1)*
Surf. Sci. 415 (1998) 212

[Yau96] S.-L. Yau, Y.-G. Kim, K. Itaya
*In situ scanning tunneling microscopy of benzene adsorbed on Rh(111) and Pt(111) in HF solution*
J. Am. Chem. Soc. 118 (1996) 7795

[Yos95] J. Yoshinobu, H. Tanaka, M. Kawai
*Elucidation of hydrogen-induced (1x2) reconstructed structures on Pd(110) from 100 to 300 K by scanning tunneling microscopy*
Phys. Rev. B 51 (1995) 4529

[Zan88] A. Zangwill
*Physics at surfaces*
Cambridge University Press, Cambridge (1988)

[Zei83] M.S. Zei, Y. Nakai, G. Lehmpfuhl, D.M. Kolb
*The structure of gold and silver films evaporated on glass. A LEED and RHEED study*
J. Electroanal. Chem. 150 (1983) 201

[Zei94] M.S. Zei, N. Batina, D.M. Kolb
*On the stability of reconstructed Pt(100) in an electrochemical cell: an ex-situ LEED/RHEED and in-situ STM study*
Surf. Sci. 306 (1994) L519

[Zei97] M.S. Zei, G. Ertl
*Electrodeposition of Cu onto reconstructed Pt(100) and Pt(110) surfaces*
Z. Phys. Chem. 202 (1997) 5

[Zei00] M.S. Zei, G. Ertl
*Structural changes of a Ru(0001) surface under the influence of electrochemical reactions*
Phys. Chem. Chem. Phys. 2 (2000) 3855.

[Zel91] P. Zelenay, G. Horányi, C.K. Rhee, A. Wieckowski
*Voltammetric and radioactive labeling studies of single crystal and polycrystalline rhodium electrodes in sulfate-containing electrolytes*
J. Electroanal. Chem. 300 (1991) 499

[Zou98] S. Zou, R. Gómez, M. Weaver
*Infrared spectroscopy of carbon monoxide at the ordered palladium (110)-aqueous interface: evidence for adsorbate-induced surface reconstruction*
Surf. Sci. 399 (1998) 270

[Zur87] D. Zurawski, L. Rice, M. Hourani, A. Wieckowski
*The in-situ preparation of well-defined single crystal electrodes*
J. Electroanal. Chem. 230 (1987) 221

## 8. Acknowledgements

The author is most grateful to Prof. Dr. Dieter M. Kolb, who reviewed the manuscript and continuously motivated the idea of having a course on single crystal preparation. Any suggestions that readers may have for improvement of this booklet are very much welcome.